NUREG/CR-4728
SAND86-1938
RV
Printed February 1988

Equipment Qualification Research Test of a High-Range Radiation Monitor

E. H. Richards, M. J. Jacobus, P. M. Drozda, J. A. Lewin

Prepared by
Sandia National Laboratories
Albuquerque, New Mexico 87185 and Livermore, California 94550
for the United States Department of Energy
under Contract DE-AC04-76DP00789

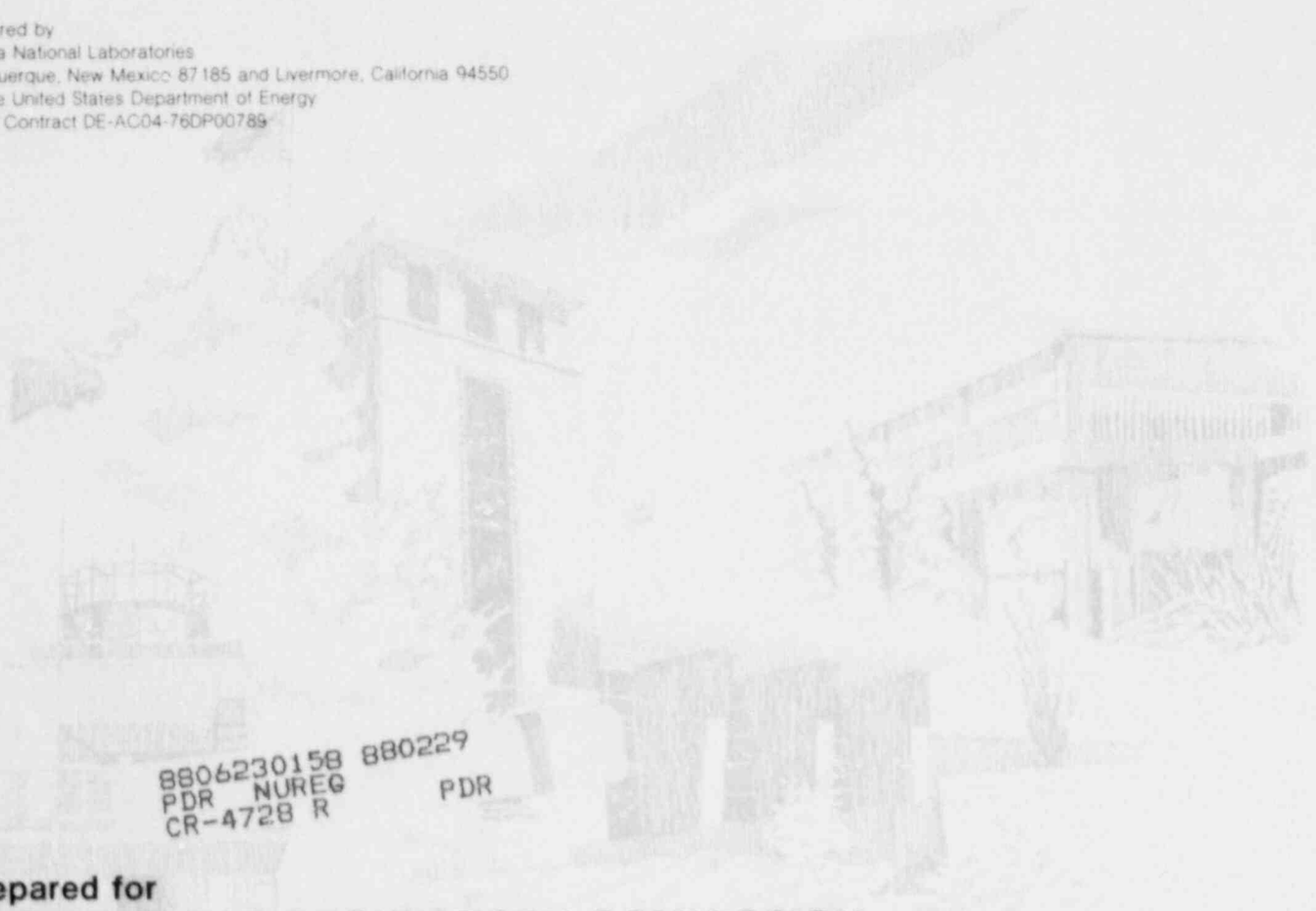

8806230158 880229
PDR NUREG PDR
CR-4728 R

Prepared for
U. S. NUCLEAR REGULATORY COMMISSION

SF2900Q(8-81)

NOTICE

This report was prepared as an account of work sponsored by an agency of the United States Government. Neither the United States Government nor any agency thereof, or any of their employees, makes any warranty, expressed or implied, or assumes any legal liability or responsibility for any third party's use, or the results of such use, of any information, apparatus product or process disclosed in this report, or represents that its use by such third party would not infringe privately owned rights.

Available from
Superintendent of Documents
U.S. Government Printing Office
Post Office Box 37082
Washington, D.C. 20013-7082

and

National Technical Information Service
Springfield, VA 22161

NUREG/CR-4728
SAND86-1938
RV

EQUIPMENT QUALIFICATION RESEARCH TEST OF A HIGH-RANGE RADIATION MONITOR

E. H. Richards
M. J. Jacobus
P. M. Drozda
J. A. Lewin

February 1988

Sandia National Laboratories
Albuquerque, NM 87185
operated by
Sandia Corporation
for the
U. S. Department of Energy

Prepared for
Electrical and Mechanical Engineering Branch
Division of Engineering
Office of Nuclear Regulatory Research
U. S. Nuclear Regulatory Commission
Washington, DC 20555
Under Memorandum of Understanding DOE-40-550-75
NRC FIN No. A-1051

Abstract

A high-range radiation detector was tested in a simultaneous steam and radiation environment simulating a postulated loss-of-coolant accident (LOCA) to assess possible synergistic effects that may be important to its performance in an accident. The detector, manufactured by General Atomic, was simultaneously subjected to a simulated accident environment including 171°C (340°F) steam at 410 kPa gage (60 psig) and 4 Mrad/hr gamma radiation while its performance was monitored. Test results showed that the detector successfully operated at the high dose rate and temperature, without evidence of synergisms. However, at reduced radiation levels in a saturated steam environment, the detector signal at the readout module deteriorated in accuracy or ceased altogether. The cause of these anomalies is attributed to leakage currents and/or possible galvanic action in the coaxial connections and/or cables.

Table of Contents

Executive Summary..... 1

1. Introduction..... 3
   1.1 Test Objective..... 3
   1.2 Background..... 3
   1.3 Scope..... 4

2. Test Specimen..... 5
   2.1 Specimen Description..... 5
   2.2 Basis for Selection..... 6

3. Test Description..... 7
   3.1 Test Facility..... 7
      3.1.1 HIACA..... 7
      3.1.2 Steam System..... 7
      3.1.3 Test Chamber..... 7
      3.1.4 Instrumentation..... 11
   3.2 Test Environment..... 12
      3.2.1 Aging..... 12
      3.2.2 Accident Simulation..... 13
      3.2.3 Dry run tests..... 15
   3.3 Monitoring of Test Specimen..... 17
      3.3.1 Pretest Characterization..... 17
      3.3.2 Functional Performance During Test..... 17
         3.3.2.1 Output Signal..... 17
         3.3.2.2 Insulation Resistance..... 18
         3.3.2.3 Effect of Cable Length..... 18
      3.3.3 Post-test Characterization..... 18
      3.3.4 Acceptance Criteria..... 18

4.0 Test Results..... 20

5.0 Analysis of Test Results..... 38
   5.1 Data from Bench Tests..... 38
   5.2 Analysis of Data from Bench Test..... 40

6.0 Conclusions and Recommendations..... 46
   6.1 Detector Performance..... 46
   6.2 Recommendations for Radiation Monitor Users.... 46
   6.3 Recommendations for Future Tests..... 47

7.0 References..... 48

APPENDIX A Discussion of Split in Cable Jacket..... 49

List of Figures

Figure 1.	RD-23 Detector	5
Figure 2.	Radiation Film Detectors used to Calibrate HIACA	8
Figure 3.	Test Chamber Installed in HIACA Facility	9
Figure 4	Mounting Fixture for RD-23 Detector	10
Figure 5.	Thermocouple Locations	12
Figure 6.	LOCA Environment Profile, Based on IEEE323-1974	13
Figure 7.	Dose Rates Calculated from IEEE323-1974, Table A1	14
Figure 8.	Dose Rate Comparison: HIACA vs. IEEE323-1974	16
Figure 9.	Dummy Test Specimen	16
Figure 10.	Chamber Pressure and Temperature and Detector Output	21
Figure 11.	Detector Output at Beginning of Test	31
Figure 12.	Strip Chart Record of Detector Output	34
Figure 13.	Block Diagram of Operational Amplifier Circuit	41

List of Tables

Table 1. Dose Rates for HIACA Co-60 Groups..... 11
Table 2. IEEE 323-1974 Radiation Profile (PWR)..... 14
Table 3. HIACA Dose Rate Profile Used for Test..... 15
Table 4. Calibration Data..... 32
Table 5. Cable Insulation Resistance During Test..... 36
Table 6. Experimentally Determined Outputs of the Readout Module for Various Insulation Resistances and Input Currents..... 39

Acknowledgments

The authors would like to thank Lloyd Bonzon for his assistance in planning this test program; Tim Gilmore, Ron Garcia, Bob Padilla, and Craig Ginn for assisting in the execution of the test; Frank Wyant for supplying the radiation dose rate calibration used in the test; and Jeremy Sprung for providing information on the timing of the radiation profile.

Executive Summary

A high-range radiation detector was tested in a simultaneous steam and radiation environment simulating a postulated loss-of-coolant accident (LOCA) to assess possible synergistic effects that may be important to its performance in an accident. The detector, a General Atomic model RD-23, was simultaneously subjected to a simulated reactor accident environment including 171°C (340°F) steam at 410 kPa gage (60 psig) and 4 Mrad/hr gamma radiation while its performance was monitored.

The original concern was that the heating induced by the high radiation levels would cause the ion chamber to overheat when applied simultaneously with the LOCA steam environment. Such effects would go undetected during typical qualification tests, which do not employ simultaneous exposures. We found that the detector operated successfully without any evidence of synergisms at high dose rates while exposed to the most severe environmental conditions. However, at reduced radiation levels in a saturated steam environment, the detector signal at the readout module deteriorated in accuracy or ceased altogether.

We at first believed that leakage currents in the cables and/or connections caused the anomalies, so we conducted additional electrical tests after completion of the LOCA simulation to assess the response of the readout module to variations in the insulation resistance of the interconnections. These tests demonstrated that the insulation resistance is critical at low radiation dose rates, but becomes less significant as the dose rate is increased.

The tests also established that the loss of signal at the readout module, manifested by the readings going off-scale at the low end of the range, was not caused by decreased insulation resistance. We found that the effects of decreased insulation resistance, both as determined by theoretical considerations as well as by test data, would have caused our particular detector to read abnormally high. The only explanation we could postulate for the detector's behavior during the LOCA simulation was galvanic action in the coaxial connections and/or cables, although we were unable to confirm this theory.

The results indicate that "low" dose rates cannot be accurately measured under the conditions used in this test. However, higher dose rates can be monitored accurately even though the green "operate" light on the readout module may go off prior to the presence of high dose rate radiation. (If the light does go off, resetting the light illuminates it again.)

We concluded that

a) At low radiation dose rates, insulation resistance effects of the interconnections may cause detector accuracy to

degrade beyond the factor of two allowed by Regulatory Guide 1.97. The magnitude and direction of the observed error depend on the interconnection insulation resistance, the readout module input amplifier's input offset voltage, and the detector signal level.

b) A second effect, perhaps galvanic action, caused the detector signal to be lost at low levels of detector output. We were unable to hypothesize any other mechanism which would explain the observed loss of signal during the accident test. We also noted that for our test, whatever this effect was, it appeared to dominate at low detector currents. After the test, we discovered a small split in the cable jacket which may have provided a convenient path for moisture intrusion, facilitating a galvanic reaction (although some moisure intrusion through the cable jacket would be expected even without the split).

We recommend that users of the RD-23 detector assess the results of this test program as it relates to their detector installation. We also recommend that licensees with other types of high-range radiation detectors review their qualification test data to check for similar concerns.

1. Introduction

1.1 Test Objective

The purpose of this testing program was to investigate synergistic effects of Loss-of-Coolant Accident (LOCA) steam conditions and high level radiation environments on a high-range radiation detector. The test was designed to assess the importance of qualifying high-range radiation detectors using simultaneous LOCA and radiation exposures as opposed to qualifying the detectors using sequential exposures. We were concerned that the high radiation dose rates early in an accident might cause excessive radiation heating when coupled with the LOCA steam conditions, causing damage to the detector. The test was not run with the intent of duplicating the vendor qualification test, but rather to subject the detector to a more representative design basis accident environment than that generally used during qualification. Specifically, the radiation detector was exposed simultaneously to a LOCA steam environment and a radiation profile representative of a design basis accident. By comparison, typical qualification tests include irradiation of a piece of equipment to a given dose (usually at a much lower dose rate than that predicted for peak accident conditions) followed by exposure to a LOCA steam environment (i.e., sequential testing).

1.2 Background

The Nuclear Regulatory Commission (NRC), via NUREG-0737[2] and Regulatory Guide (RG) 1.97,[1] sets forth requirements for monitoring radiation levels after an accident at a nuclear power generating station. One of the requirements specifies that plants must have at least two high-range radiation detectors installed in containment to monitor the high levels (greater than 10^6 rad/hr) of radiation associated with accidents. It is further required that these detectors or monitors be Class 1E qualified to withstand the LOCA and radiation environments. Based on our knowledge of plant installations from equipment qualification inspections, three manufacturers' detectors have been tested and installed in plants. None of these detectors were qualified using simultaneous exposures of radiation and the LOCA environment.

Questions have been raised regarding possible synergistic effects of the LOCA and high radiation environments. An NRC memorandum dated 11/27/84[3] requested testing of at least one high-range radiation detector using simultaneous exposures to LOCA steam and high radiation dose rates. The request was based on an NRC staff "Evaluation of Presently Installed High-Range Containment Monitors in Nuclear Power Reactors," (included with the memorandum). The evaluation's primary concern stemmed from an article in Health Physics.[4] In the article, the authors calculated a significant temperature rise

for gas-filled radiation detectors (such as gas ionization chambers) when exposed to high levels of radiation. The staff was concerned that this temperature rise, if it actually occurs, combined with a LOCA steam exposure temperature could cause thermal damage or failure of the detector. Such effects would go undetected during qualification tests which do not employ simultaneous exposures.

Other types of failures not due to synergistic effects were also possible, such as failures due to moisture intrusion or other consequences of the steam environment alone. In addition, although we were primarily interested in the detector's response, the monitoring system cannot function unless the cable and connections also survive the accident conditions.

As it turned out, while the system operated satisfactorily at the high dose rates, it experienced some anomalous behavior at lower dose rates. We believe this anomalous behavior was not a result of any synergistic effects, but was a result of the response of the cable and/or connections to the LOCA steam environment.

1.3 Scope

This report covers testing of an unaged General Atomic (GA) RD-23 radiation detector which was exposed to accident radiation doses and dose rates simultaneously with the LOCA steam environment. Again, the intent of the test was not to qualify the detector by putting it through the standard set of qualification tests used in the industry, but to understand how it responds to a more realistic simulation of a design-basis accident environment. Sprays were not simulated in the test.

The test plan[5] originally projected additional tests of the same detector, as well as other detectors, depending on the results obtained from the test documented here. However, while the detector signal reaching the readout module did experience some anomalous behavior, the anomalies do not appear to be the result of a synergistic effect on the detector itself. Based on the results of this test and discussions with the NRC, we do not see a need for further testing of the RD-23. We believe that the test anomalies were due to the cable and/or connections and that it would be more beneficial to direct future studies toward examining the behavior of coaxial cables and connections. A radiation monitor might be needed in such a test to produce and monitor the low level signals associated with the overall system.

2. Test Specimen

2.1 Specimen Description

The item tested was General Atomic's model RD-23 radiation detector, a gas ionization chamber, which is part of GA's model RS-23 high-range radiation monitoring system. The RS-23 system can be purchased as either an analog or digital system. We purchased one complete RS-23 analog system (RS-23A) with one RD-23 gamma detector.

A diagram (taken from GA promotional literature[6]) of the RD-23 radiation detector is shown in Figure 1. It consists of a gas ionization chamber, stainless steel housing, integral cables, connections, and pull box with cover. The ionization chamber has two integral mineral-oxide insulated cables, one for signal, the other for high voltage. LOCA-qualified connections are included for connecting the in-containment cables to the integral cables. The ionization chamber is electrically isolated from the detector housing to minimize noise and is mechanically isolated from the detector housing to protect it from thermal and mechanical shock. A more detailed drawing can be obtained from References 7 and 8; a proprietary information agreement prevents us from including it here.

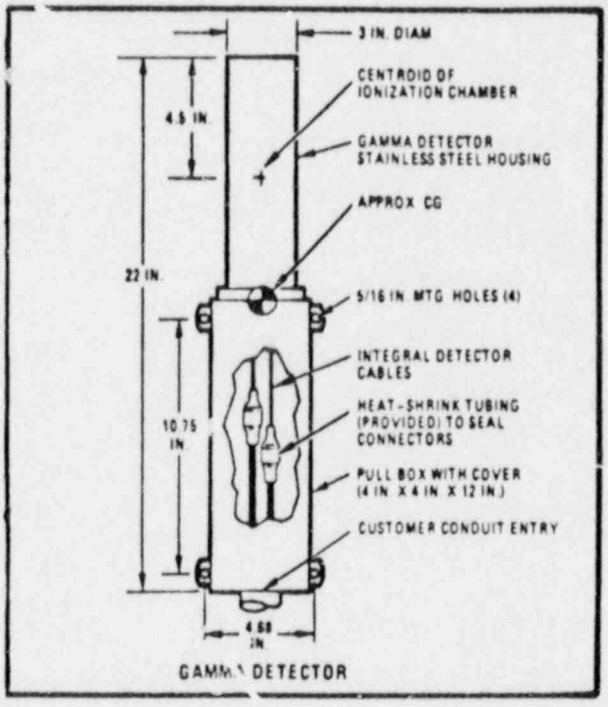

Figure 1. RD-23 Detector.

During operation, gamma radiation inside containment is sensed by the RD-23 detector. The ionization chamber produces a direct current proportional to the gamma flux. The current travels over coaxial cable, is sensed by a log picoammeter that is temperature-compensated to minimize drift, and is displayed in roentgens per hour on the front panel meter. To maintain a signal at all times, a coating of U-234 is applied to the inside of the ion chamber housing. This generates a sustained signal within the detector corresponding to approximately 1 rad/hr. A failure alarm will occur if the signal from the detector falls (sufficiently) below this value. This feature is intended to assure knowledge of the monitor's integrity at all times. Detailed information concerning the RD-23's

specifications, installation, and operation can be obtained in References 6, 7, and 8.

The GA requirements for interconnecting the detector specify that a cable with an insulation resistance of at least 10^9 ohm be used. Similar requirements are specified for the electrical penetration, with even more stringent requirements if the detector is expected to operate under station fault conditions. As can be shown using the equation developed in Section 5.2, an insulation resistance of 5×10^8 ohm (accounting for 10^9 ohm for the cable and interconnections and 10^9 ohm for the penetration, connected in parallel) will maintain the overall instrument accuracy within the factor of two allowed by RG 1.97[1] if a reasonable worst case amplifier offset voltage is assumed and if other effects are neglected. The error due to any given insulation resistance will be shown to be a function of the combined (parallel) insulation resistances of all interconnecting devices, the detector signal level, and the input offset voltage of the readout module input operational amplifier.

2.2 Basis for Selection

We chose to test this particular radiation detector for several reasons. One is that, based on equipment qualification inspections and the EPRI Equipment Qualification Data Bank,[9] this model is currently installed in many reactor containments. GA has LOCA qualified the RD-23 to IEEE 323-1974,[10] and claims that the monitor meets the requirements of RG 1.97. Another reason for testing the RD-23 is that the dimensions of this particular detector are such that it will fit into the size test chamber required to achieve the high dose rates in Sandia's test facility.

3. Test Description

3.1 Test Facility

3.1.1 HIACA

The accident simulation tests took place in Sandia's High Intensity Adjustable Cobalt Array (HIACA). A complete description of the HIACA is available in Reference 11; it will be described only briefly here.

The HIACA consists of 32, 24-in. Cobalt-60 source pencils. The pencils are arranged in a circle or circles, giving a cylindrical test volume that supplies a uniform dose to test specimens, thus eliminating the need to rotate samples to obtain uniform exposure. The array is adjustable: the pencils can be moved to accommodate larger test specimens at lower dose rates or smaller specimens at higher dose rates. The facility design also allows the source to be configured either one or two pencils high. For this test, the smallest radius was used with the 24-in pencil configuration to obtain dose rates up to about 4 Mrad/hr. (Throughout this report, all dose rates are reported in rad/hr (air) or Mrad/hr (air). The detector output actually reads in R/hr, but the two are equivalent.)

Before installing the detector in the HIACA, we calibrated the radiation levels using film detectors (Figure 2). Table 1 shows the average radiation dose rates for the different groups of rods in the configuration used in the test.

3.1.2 Steam System

Sandia has the capability of being able to apply the LOCA steam exposure and the accident radiation dose simultaneously. The steam system is designed to accommodate severe accident testing; the test of the radiation detector did not require such extreme conditions, and the facility had no trouble meeting the desired conditions. The boiler shut down once during the test, but the associated temporary drop in pressure should not affect the test results.

3.1.3 Test Chamber

Figure 3 shows the test chamber installed in the test facility. It was constructed using a stainless steel pipe with a standard pipe end cap forming the bottom. The RD-23 detector was installed in the test chamber via a mounting fixture attached to the chamber head (Figure 4). The simplest way to mount the detector would have been to mount it upside down in the chamber so that the cable (which exits the detector through the bottom) would not have to be doubled back to penetrate the test vessel. The installation instructions for the detector do not specify that the detector be mounted in a particular

Figure 2. Radiation Film Detectors used to Calibrate HIACA.

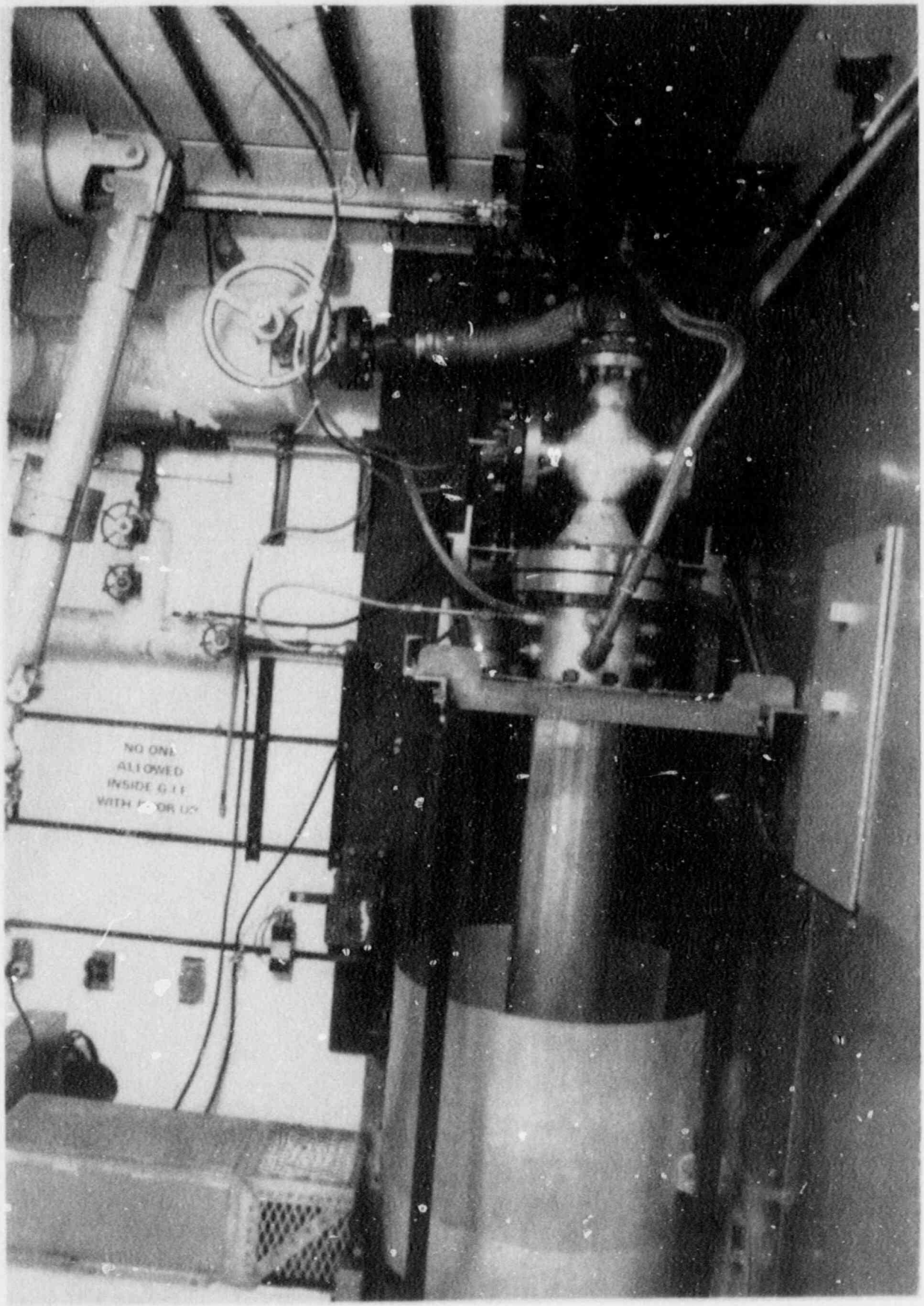

Figure 3. Test Chamber Installed in HIACA Facility.

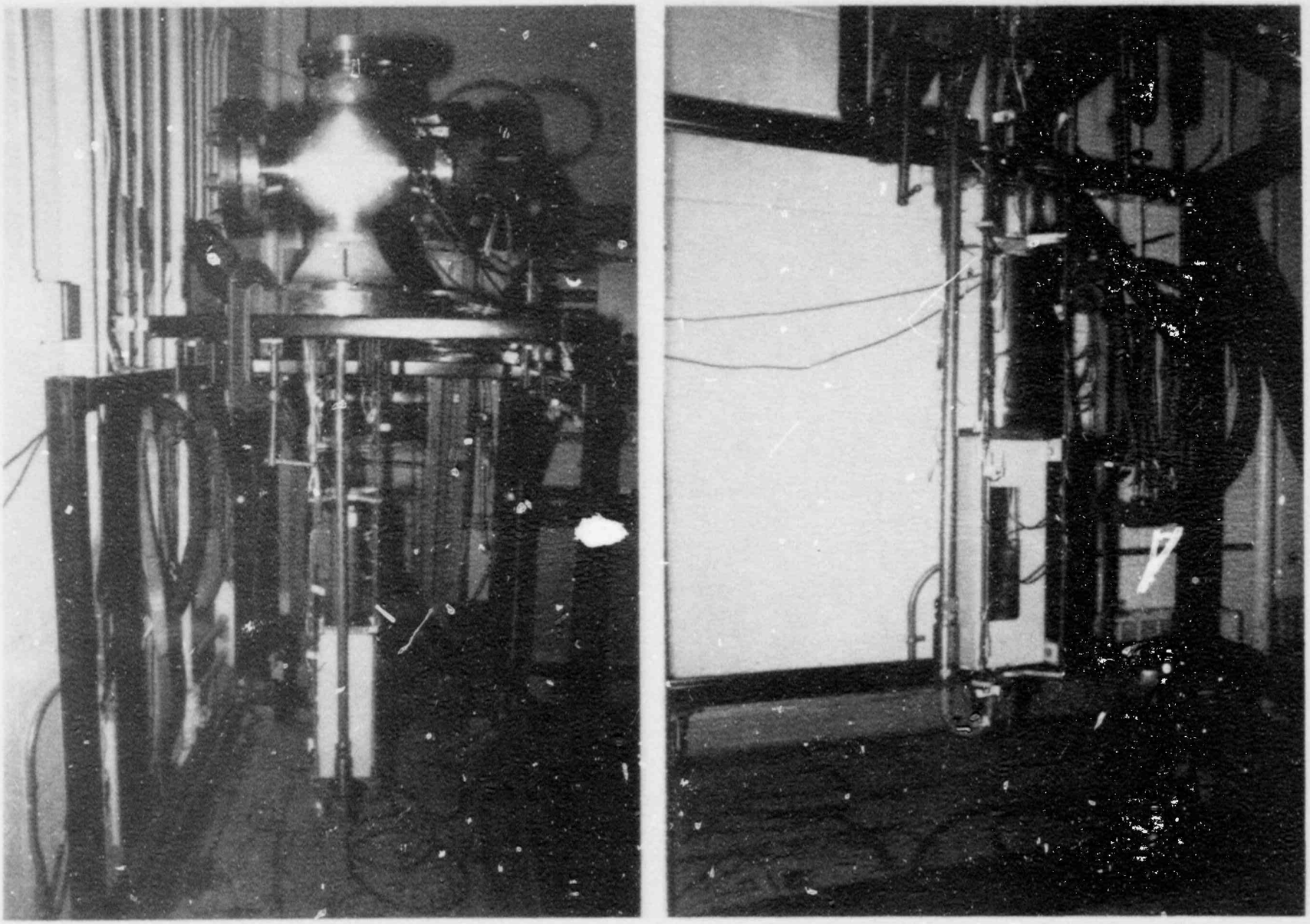

Figure 4. Mounting Fixture fo RD-23 Detector.

Table 1. Dose Rates for HIACA Co-60 Groups.

Group	Calculated (Mrad/hr)	Measured (Mrad/hr)
1 *	0.19	0.13
2	0.66	0.61
3	0.21	0.15
4	0.63	0.58
5	0.20	0.14
6	0.64	0.59
7	0.19	0.13
8	0.61	0.56

* To determine the dose rate from a combination of groups, sum the calculated values, then determine the corresponding actual value from the equation

$$\dot{D}_A = 1.015\left(\sum \dot{D}_C\right) - 0.060$$

orientation. However, information from NRC Office of Inspection and Enforcement inspections indicated that the in-service orientation of the detector may be important because the detector was qualified for sprays "right-side-up." Therefore, the detector was tested right-side-up, with the cable doubled back to the chamber penetrations. Because we were interested in the detector performance, not the cable performance, most of the cable was enclosed in sealed conduit to protect it as well as possible during the test (the short cable segment in the detector junction box was exposed to the environment).

We were very careful to follow the instructions[7,8] provided with the detector to ensure that its Class 1E qualification was not compromised during installation. The instructions are the same as those provided to the utilities, and include directions for installing, connecting, and operating the detector.

3.1.4 Instrumentation

Pressure and temperature instrumentation were employed to monitor the test conditions given in Section 3.2, and the output of the test specimen was recorded digitally as well as with a strip chart recorder. The analog monitor provided with the detector also provided a visual indication of the detector output. The test facility is equipped with a variety of data acquisition systems capable of monitoring and recording the necessary pressures, temperatures, ramp times, and other pertinent data. The instrumentation channels for monitoring the test specimen's response were on a separate data acquisition system from the environmental monitoring. Both

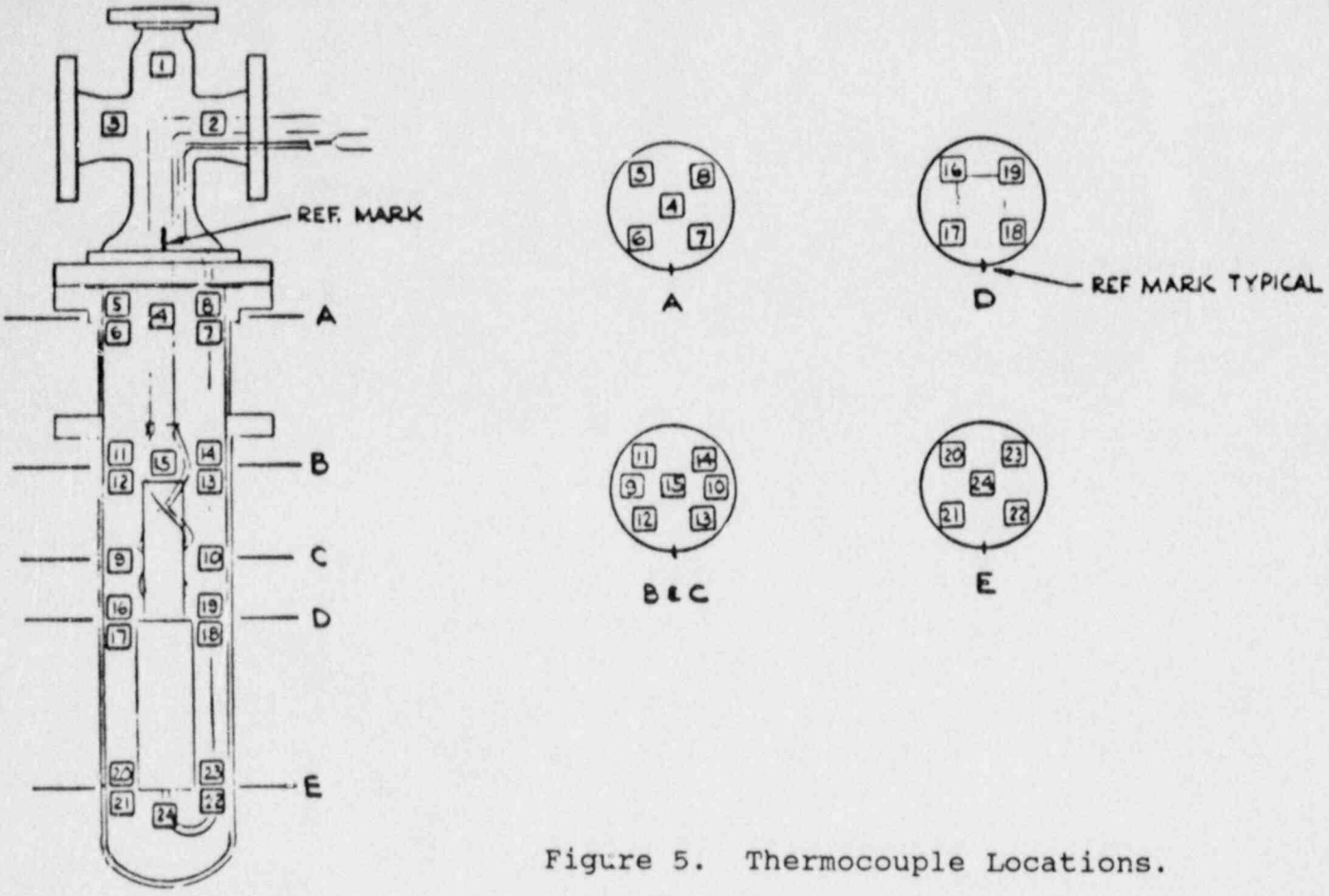

Figure 5. Thermocouple Locations.

acquisition systems were connected to a computer to facilitate analysis.

Figure 5 shows the locations of the thermocouples used to monitor the temperature inside the chamber. We computed average chamber temperatures using thermocouple numbers 9 through 19 and 9 through 24. The first average indicated how the temperature immediately around the ionization chamber compared with the overall chamber average. We used the second average to control the environment in the chamber; it is also the chamber temperature reported in the figures in section 4. The two averages compared well, differing by only about a degree throughout the test. It did not prove feasible to mount thermocouples inside the detector to monitor the temperature of the ionization chamber, as we did not want to interfere with its Class 1E qualification status.

3.2 Test Environment

3.2.1 Aging

The test specimen was not aged in this test. There are no age sensitive materials in the detector itself; the only such

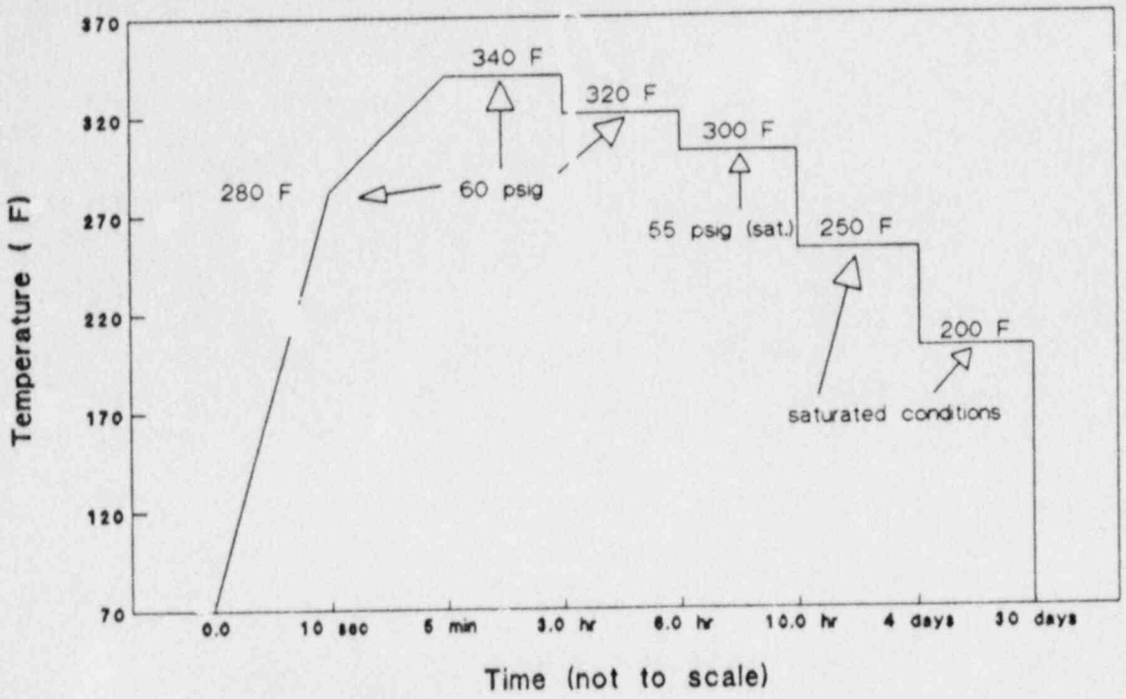

Figure 6. LOCA Environment Profile, Based on IEEE323-1974.

materials are contained in the Rockbestos cable and interconnections. We were most interested in the detector's behavior, and did not want the cable or connector to obscure the detector's response by failing during the test.

3.2.2 Accident Simulation

The LOCA test was based on the profile given in IEEE 323-1974, except that we used only one temperature ramp (Figure 6). Most Class 1E equipment (including high-range radiation detectors) is tested using the two-ramp profile. Most qualification programs apply radiation (aging and accident) before the LOCA steam simulation. However the intent of this test was to subject the detector to a more realistic simulation of the design-basis accident, so we applied the accident radiation dose simultaneously with the LOCA conditions. Also, most qualification programs specify a total integrated dose (TID), but do not specify accident dose rates. We simulated, within the capabilities of the test facility, the radiation profile given in IEEE 323-1974, Appendix A (Table 2 and Figure 7 in this report).

We wanted this test to be as realistic as possible within the given constraints. One of the questions we researched before the test was, "When during the LOCA profile should the maximum radiation dose rate occur?" We did not want to expose the detector to a maximum dose rate during the maximum temperature and pressure if that was not predicted to be the

Table 2. IEEE 323-1974 Radiation Profile (PWR).

IEEE 323 specification	Calculated dose rate
4 Mrad after 1 hour	4.0 Mrad/hr
20 Mrad after 12 hour	1.45 Mrad/hr
24 Mrad after 1 day	0.33 Mrad/hr
40 Mrad after 10 days	0.074 Mrad/hr
55 Mrad after 1 month	0.031 Mrad/hr
110 Mrad after 6 months	0.015 Mrad/hr
150 Mrad after 1 year	0.0092 Mrad/hr

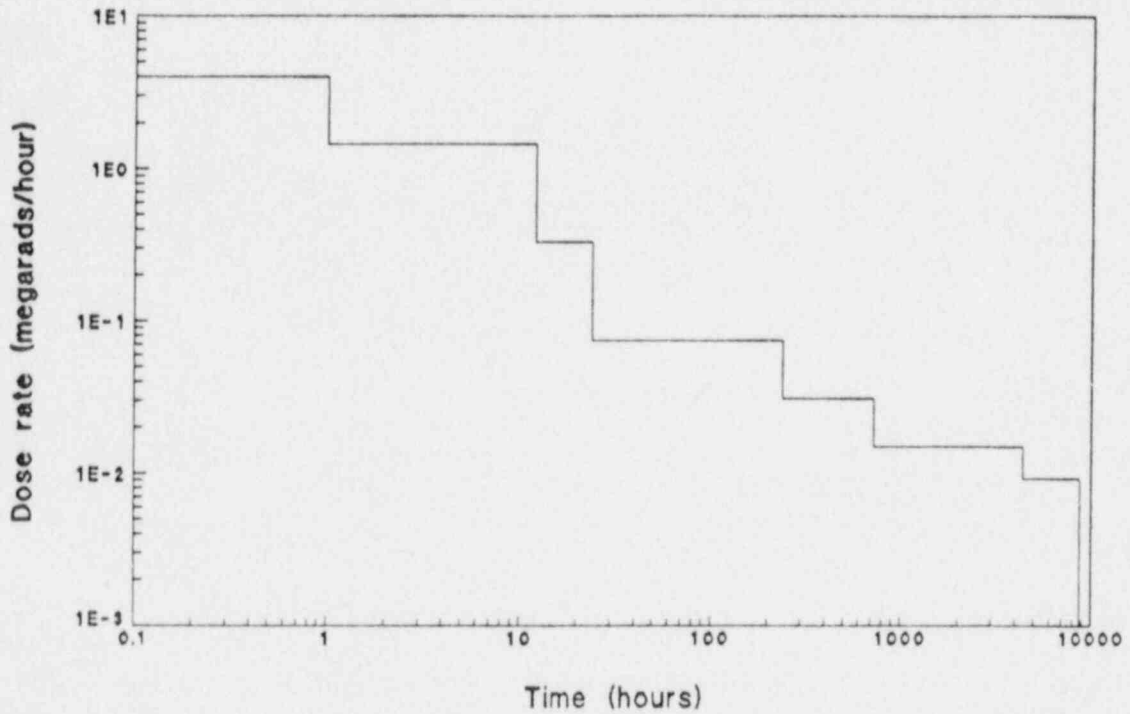

Figure 7. Dose Rates Calculated from IEEE323-1974, Table A1.

actual case during an accident. To answer the question, we looked at some results from the MARCH computer code[12]. (Note that radiation doses for design basis accidents are based on predictions of severe accident environments.) The MARCH predictions for the accident environments varied: the dose rates were predicted to peak between a few minutes and several hours after the LOCA ramp, depending on the specific plant and accident. We chose a representative time, starting the radiation profile about 15 minutes after the LOCA ramp and reaching a peak at about 50 minutes. The steam pressure and temperature were still at a maximum at this time (Figure 6).

Thus, about 15 minutes after the temperature ramp, we began stepping up the radiation dose rate to about 4×10^6

rad/hr, the maximum that the HIACA could supply, by raising the cobalt pencils up in groups. Enough time was left between groups so that the effect of the radiation dose on the detector output could be assessed. After the maximum dose rate was reached, the dose rate was stepped back down by lowering the cobalt rods in groups to simulate the radiation profile given in IEEE 323-1974[10] and achieve the total integrated dose of 150 Mrad. The radiation dose rates available in the HIACA did not match the levels calculated from IEEE 323-1974[10] exactly, so the exposure time for each dose rate was adjusted accordingly to achieve the proper TID (Table 3 and Figure 8).

Table 3. HIACA Dose Rate Profile Used for Test.

	Groups	Dose Rate (Mrad/hr)	Dose (Mrad)	Cumulative Dose (Mrad)
0-5 min	1	0.13	0.011	0.011
5-10	1,5	0.34	0.028	0.039
10-15	1,5,2	1.01	0.084	0.123
15-20	1,5,2,6	1.66	0.138	0.261
20-25	1,5,2,6,4	2.29	0.191	0.452
25-30	1,5,2,6,4,8	2.91	0.243	0.695
30-35	1,5,2,6,4,8,3	3.13	0.261	0.956
35-90	1,5,2,6,4,8,3,7	3.32	3.043	3.999
1.5-11.1 hr	1,4,7,8	1.58	15.221	19.22
11.1-145.7	1,7	0.33	44.4	63.6
6.1-30 da	3	0.15	86.4	150

Notes:

The actual radiation profile was begun about 15 minutes into the LOCA test.
The times were adjusted slightly during the actual test to account for change in dose rates during calibration checks.

3.2.3 Dry run tests

Before any testing of the actual detector took place, several "dry runs" were made to ensure that the test chamber and penetrations were adequate and that the steam environment could be simulated. A dummy test specimen (Figure 9) that duplicated the geometry and thermal mass of the test specimen was used during the dry runs to make sure the test conditions would be met in the real test. Samples of the Rockbestos coaxial cable (RSS-6-104/LD) were included to assess the effects that the steam environment might have on their ability to transmit the low-current signal. One of the cables was installed in sealed conduit (as in the real test), and one sample was directly exposed to the environment. Both samples penetrated the chamber and were connected to a current source arrangement designed to detect differences between input

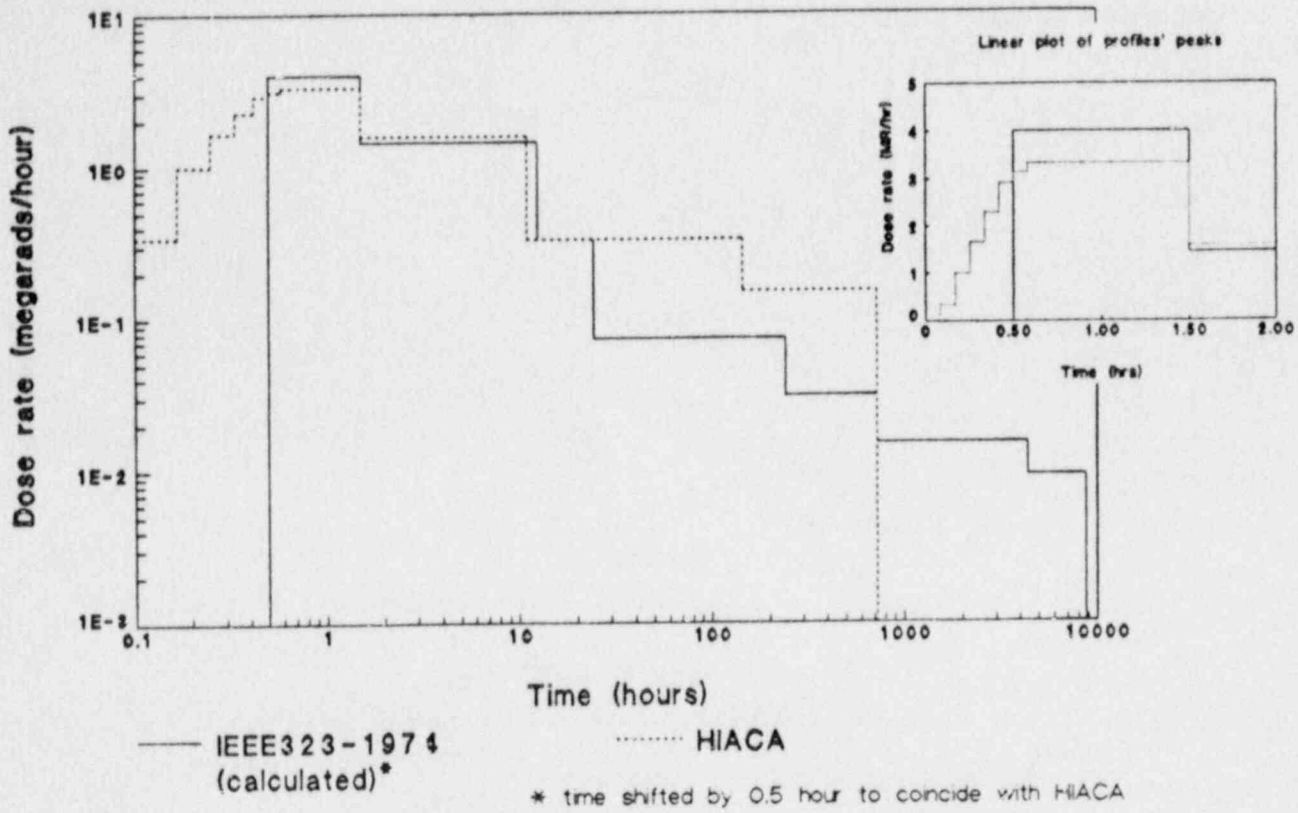

Figure 8. Dose Rate Comparison: HIACA vs. IEEE323-1974.

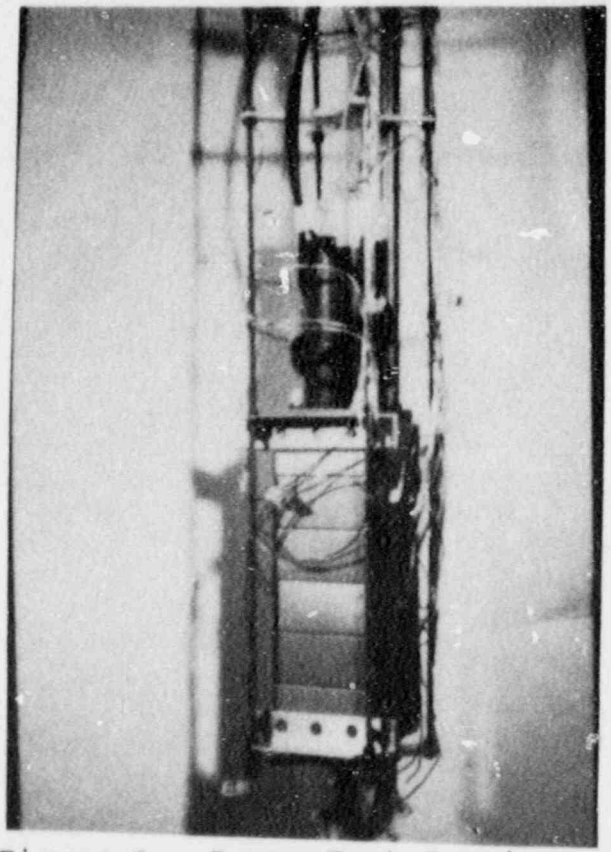

Figure 9. Dummy Test Specimen.

current and output current. No changes in signal were detected, although the insulation resistance of the cables decreased with increasing temperature as expected. We also noted that the cable's insulation extruded through the braid in some spots, a condition that may apply to other coaxial cables as well and may warrant additional investigation.

3.3 Monitoring of Test Specimen

The detector puts out an analog signal and during the test was connected to the RP-2C analog signal processor and readout module that is part of the overall GA RS-23A high-range radiation monitoring system. We recorded the readout module signal digitally with the test facility's data acquisition system, and we also used an analog strip chart recorder to facilitate execution of the test and to provide continuous data between scans by the data acquisition system. The detector output was monitored before, during, and after the LOCA steam test.

3.3.1 Pretest Characterization

After the detector was installed in the chamber and the chamber was in place in the test facility, but before the LOCA test was initiated, the cobalt rods were brought up in groups, exposing the detector to the levels of radiation it would see during the actual test. The output of the detector was recorded for each of the levels, and this information was used as a baseline comparison during the remainder of the test. This was done because the radiation calibration of the facility (see section 3.1.1) was accurate only to about 15%, and we wanted to be able to detect smaller changes in the detector's performance. Table 4 in section 4 includes these baseline radiation values. The first two entries of the calibration, 1.5 rad/hr and 218 rad/hr were obtained with the cobalt fixture elevator down and up respectively. When the elevator is down, the cobalt at the bottom of the HIACA pool gives essentially no radiation dose rate at the water surface; the 1.5 rad/hr signal is generated from the internal detector keep-alive source. When the elevator is in the up position, the cobalt source is close to the water surface and the reduced shielding leads to a dose rate of 218 rad/hr (based on the detector reading).

3.3.2 Functional Performance During Test

3.3.2.1 Output Signal

During the test, the detector monitored the level of radiation in the test chamber, and the signal was recorded both on a strip chart recorder and digitally by the data acquisition system. The RP-2C readout module also provided a visual output. The output was compared to the known levels based on

the pretest calibration measurements to determine if it was operating properly.

As shown in Table 3, the radiation test profile was lengthy; it required a given dose rate to be maintained for hours or days. This condition would only allow the detector to be checked at the existing dose rate, so we ran calibration checks to check the detector's performance over its entire range. During these checks the cobalt rods were lowered and then brought up in the prescribed sequence as done in the pretest calibration check. The calibration checks took only a short time to conduct, and we adjusted the timing of the radiation profile accordingly so that the overall dose to the detector was not significantly altered.

3.3.2.2 Insulation Resistance

During the test, the detector signal at the readout module showed some anomalous behavior at low dose rates. To try to determine the cause of this behavior, we measured the insulation resistance (IR) between the center conductor and shield of both the signal and high-voltage cables at various times during the test. For these tests, we removed the radiation, turned the power to the detector off, disconnected the detector from the readouts, and measured the IR of the cables going into the detector. The measurements were made at applied voltages of 50V, 100V, 500V, and 1000V.

3.3.2.3 Effect of Cable Length

Before the test there was some concern that, while the detector might operate satisfactorily with the relatively short cable between it and the readout, a longer cable more representative of containment applications might cause difficulty due to capacitance or insulation resistance effects. To address the capacitive effects question, we connected an additional 250 feet of cable (not exposed to the accident environment) into the system at appropriate times to determine if there was any effect on the keep-alive signal. No effects were apparent, but it should be pointed out that this small experiment does not address the cable behavior in an accident environment, which was beyond the scope of the overall test program. Further, it did essentially nothing to address the insulation resistance question (since the cable was not exposed to the harsh environment).

3.3.3 Post-test Characterization

After the LOCA exposure was complete, the rods were brought up once more, in the same order as before, to assess any change in calibration that may have occurred during or as a result of the test. After the test, the electrical characteristics of the detector were analyzed in detail (see section 5).

3.3.4 Acceptance Criteria

This was a research test, so we were most interested in how the detector behaved and why, rather than establishing Class 1E qualification. As such, we did not set specific acceptance criteria, but we did use RG 1.97[1] to assess the results. Regulatory Guide 1.97 states that the detector must be accurate within 20%, and the system (including cable, connections, readout) must be accurate within a factor of two over the entire range. The GA specifications[6] also list the system accuracy as "a factor of 2 over the entire range of the monitor." Although we attempted during the dry run tests to characterize the cable, we really did not have enough information on the connections' characteristics to evaluate whether the detector itself was within the prescribed 20%.

4.0 Test Results

Figures 10a-j show the output of the radiation detector as a function of time, along with plots of the temperature and pressure inside the chamber. Figure 10a, the first hour of the test, shows the pretest calibration of the detector (see section 3.3.1), the LOCA ramp, and the beginning of the specified radiation profile (section 3.2.2). Note the steps in the radiation profile, the result of raising up the cobalt rods in groups. (The calibration run also contains steps, but they are not evident on this time scale.) Figure 10b shows the first 12 hours of the test, Figure 10c the first 96 hours. Figures 10d-j then show the remainder of the test, in 96 hour increments. The spikes in the radiation profiles are due to the calibration checks that we made throughout the test.

Although during most of the test the detector provided an adequate measure of the radiation dose rates present in the chamber, sometimes it failed to do so, particularly at the lower dose rates. The first anomaly occurred during the pressure/temperature ramp. The HIACA elevator had not yet been brought up, so the only radiation at that time was the 1 rad/hr keep-alive signal. Figure 11 shows the erratic output of the detector during this initial portion of the LOCA exposure. Initially, coincident with the ramp, the output went high, to about 300 rad/hr, followed by a decay until the output was lost at about five minutes. It then came back and fluctuated significantly ranging from a loss of output on the low end to readings above 10^5 rad/hr at the high end (e.g., at around 0.18 hr). It disappeared again, but returned fourteen minutes into the test, when the HIACA elevator was raised to give a dose rate in the chamber of 218 rad/hr (based on the pretest calibration). It should be noted that some behavior noted in the early part of the test might have been caused by piezoelectric effects in the cable.

At this point the detector began satisfactory operation that lasted about two days. Three low-level signal checks were made during this time (by lowering the HIACA rods and elevator), one 2.2 hours into the test, one about 7 hours into the test, and one after about 30 hours. Some variation in the accuracy of the signal was evident, but the values were still very close to within a factor of two, the accuracy specified in RG 1.97[1]. The check at 7 hours gave a detector output corresponding to 3.8 rad/hr, slightly greater than a factor of two above the baseline of 1.5 rad/hr; the reading was well within a factor of two at 218 rad/hr (222 rad/hr reading). It should be noted that the LOCA conditions went from superheated to saturated between 6 and 10 hours into the test.

About 48 hours into the test, the strip chart recorded a blip in the detector signal (Figure 12a), and around 52 hours some 10% variations were evident (Figure 12b). A fourth low-level check, about 53 hours into the test, showed a loss of signal from the detector with all rods down, but the HIACA

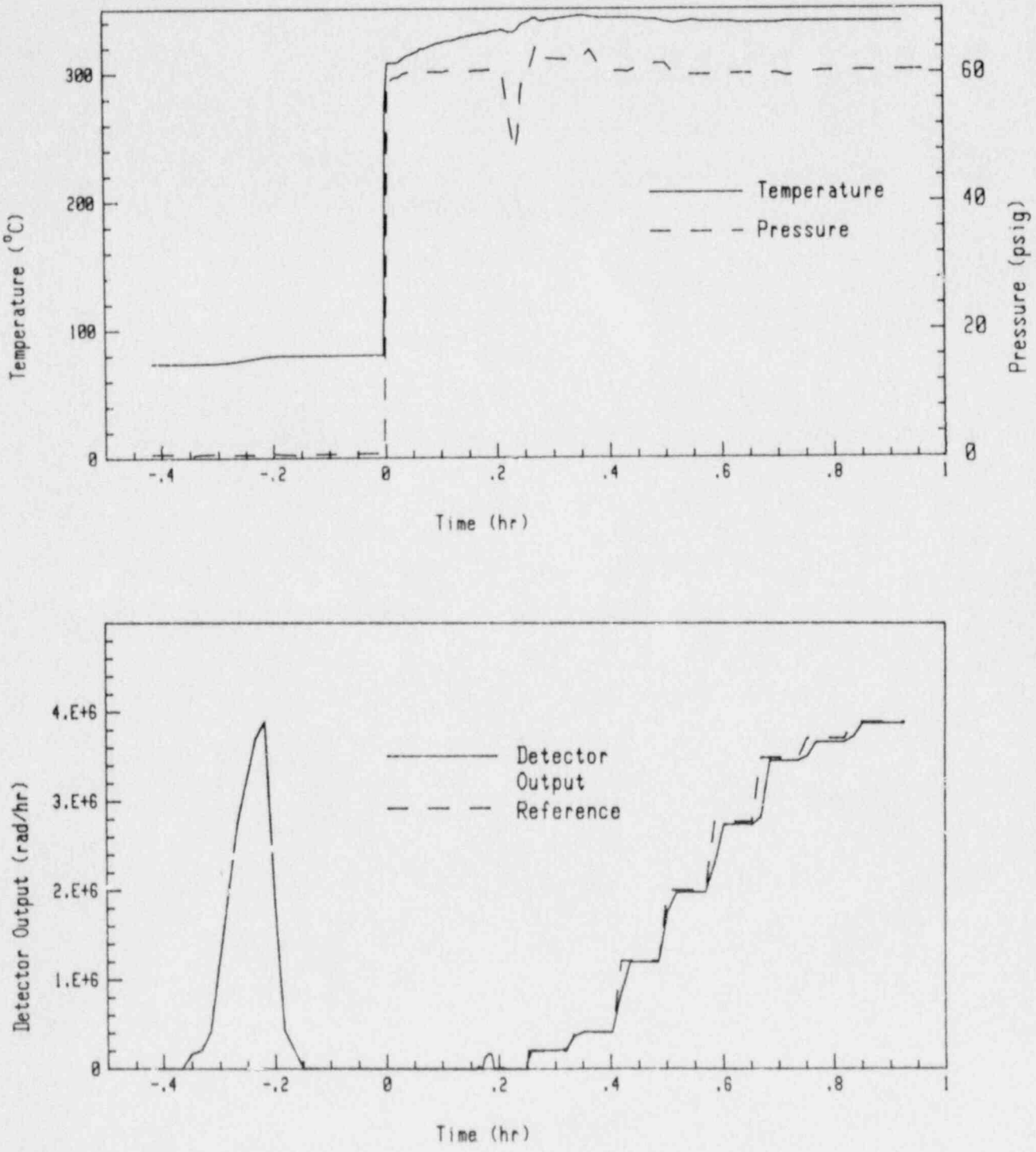

Figure 10a. Chamber Pressure and Temperature and Detector Output.

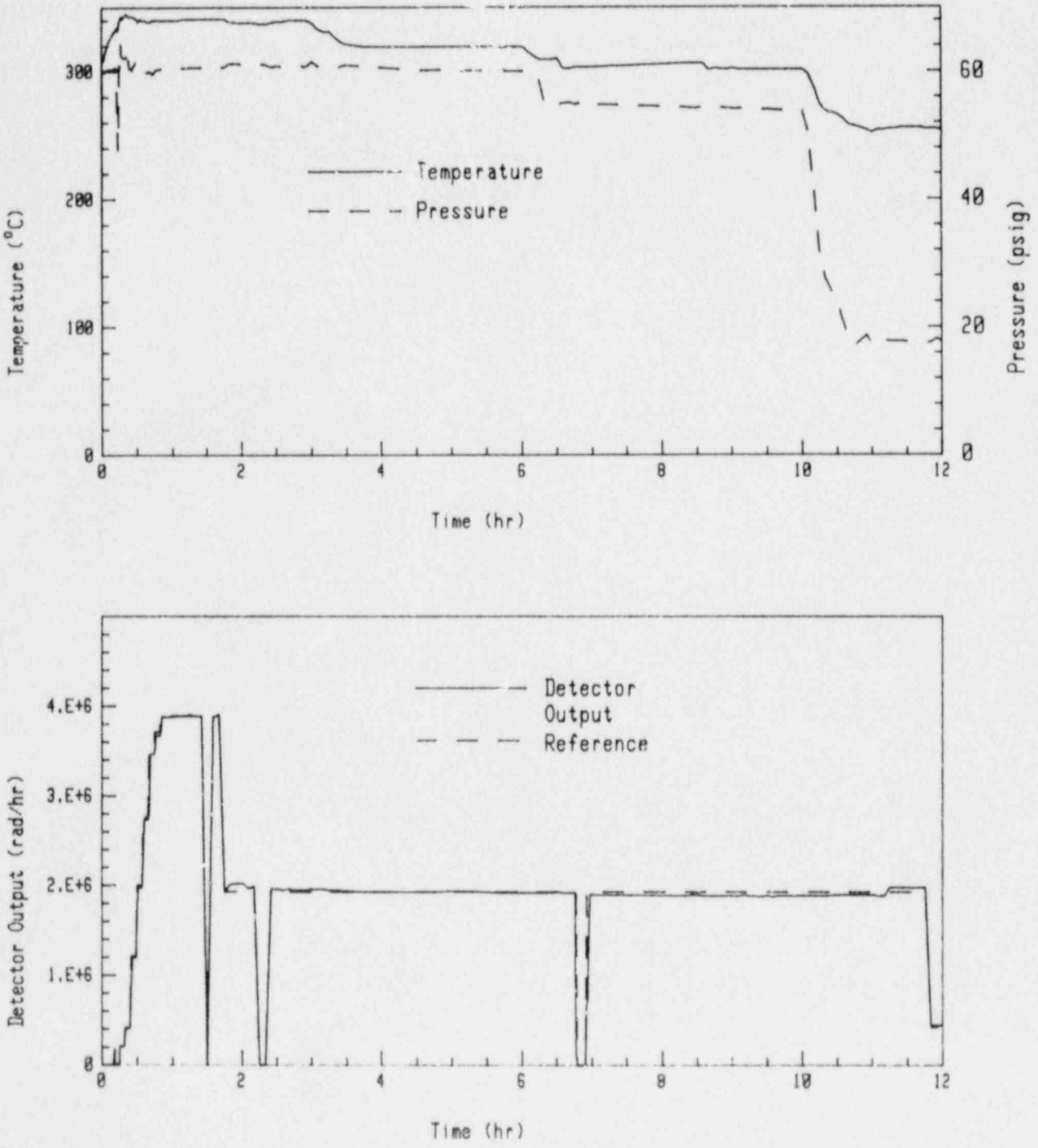

Figure 10b. Chamber Pressure and Temperature and Detector Output.

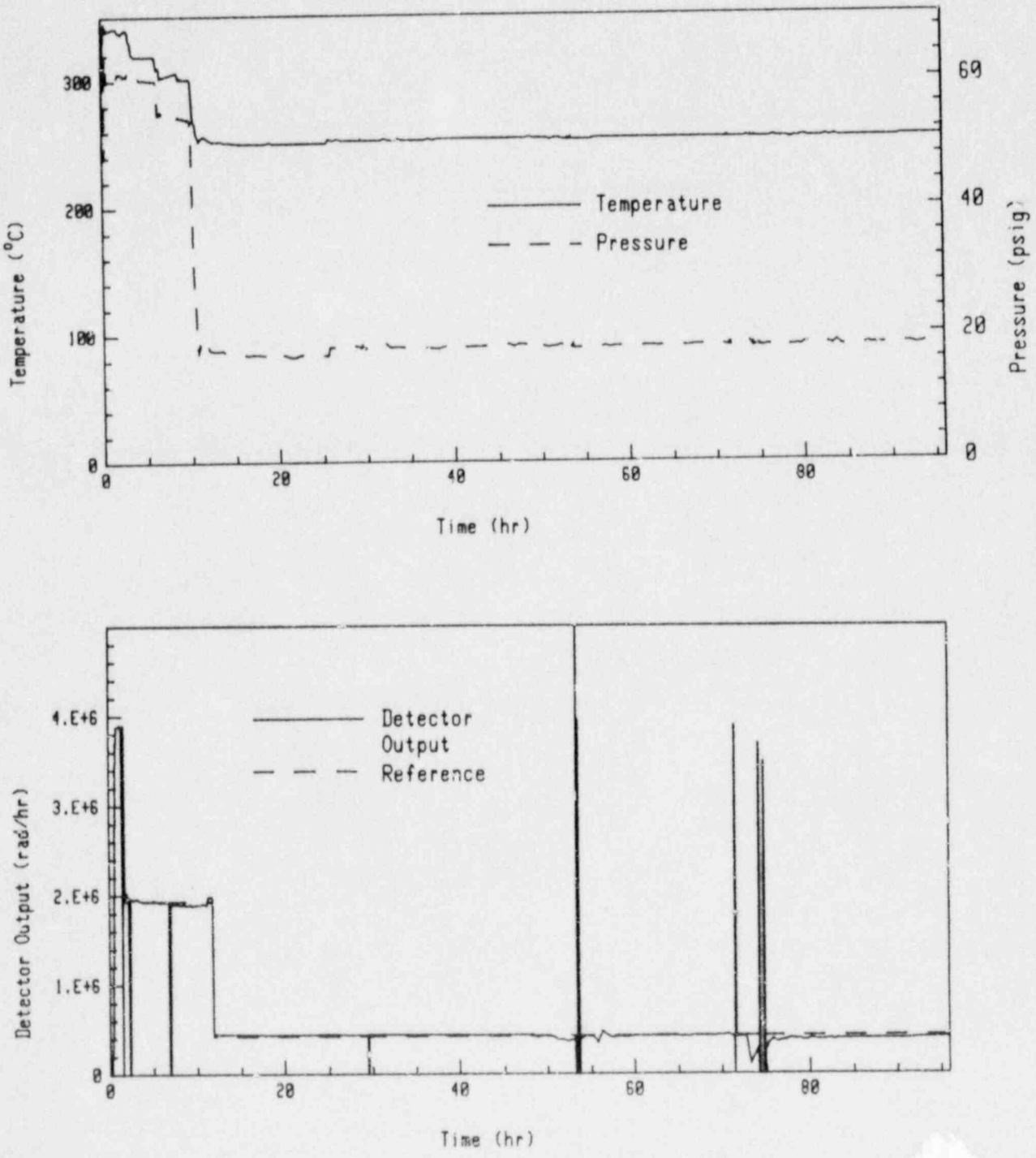

Figure 10c. Chamber Pressure and Temperature and Detector Output.

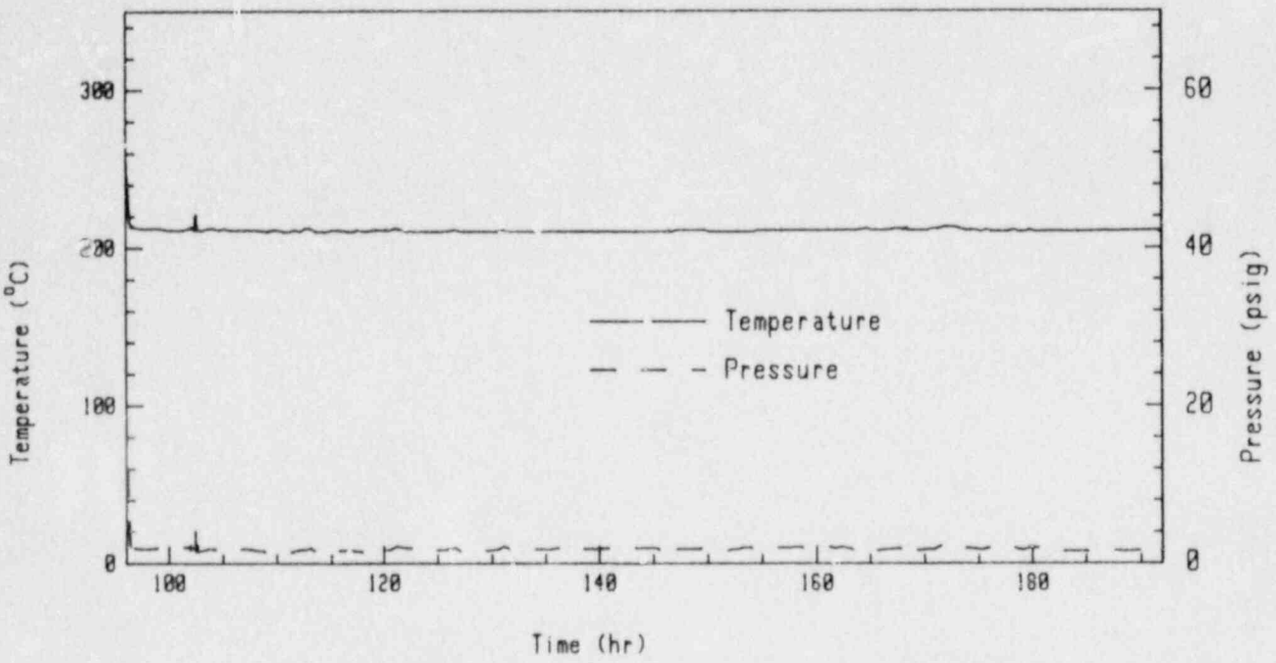

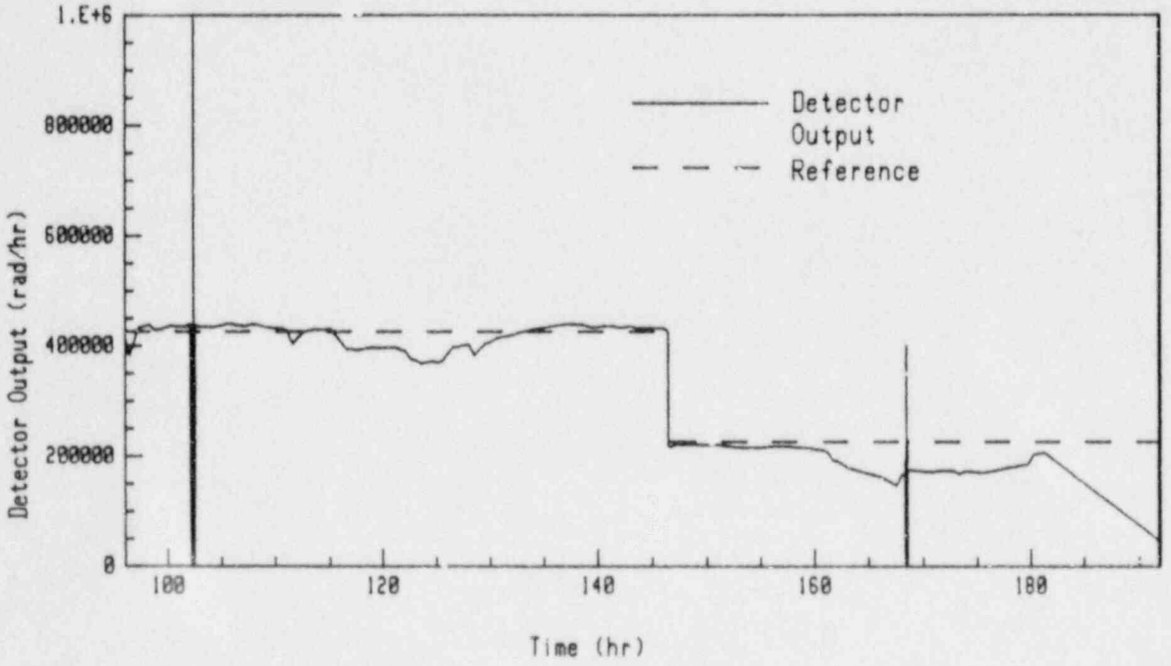

Figure 10d. Chamber Pressure and Temperature and Detector Output.

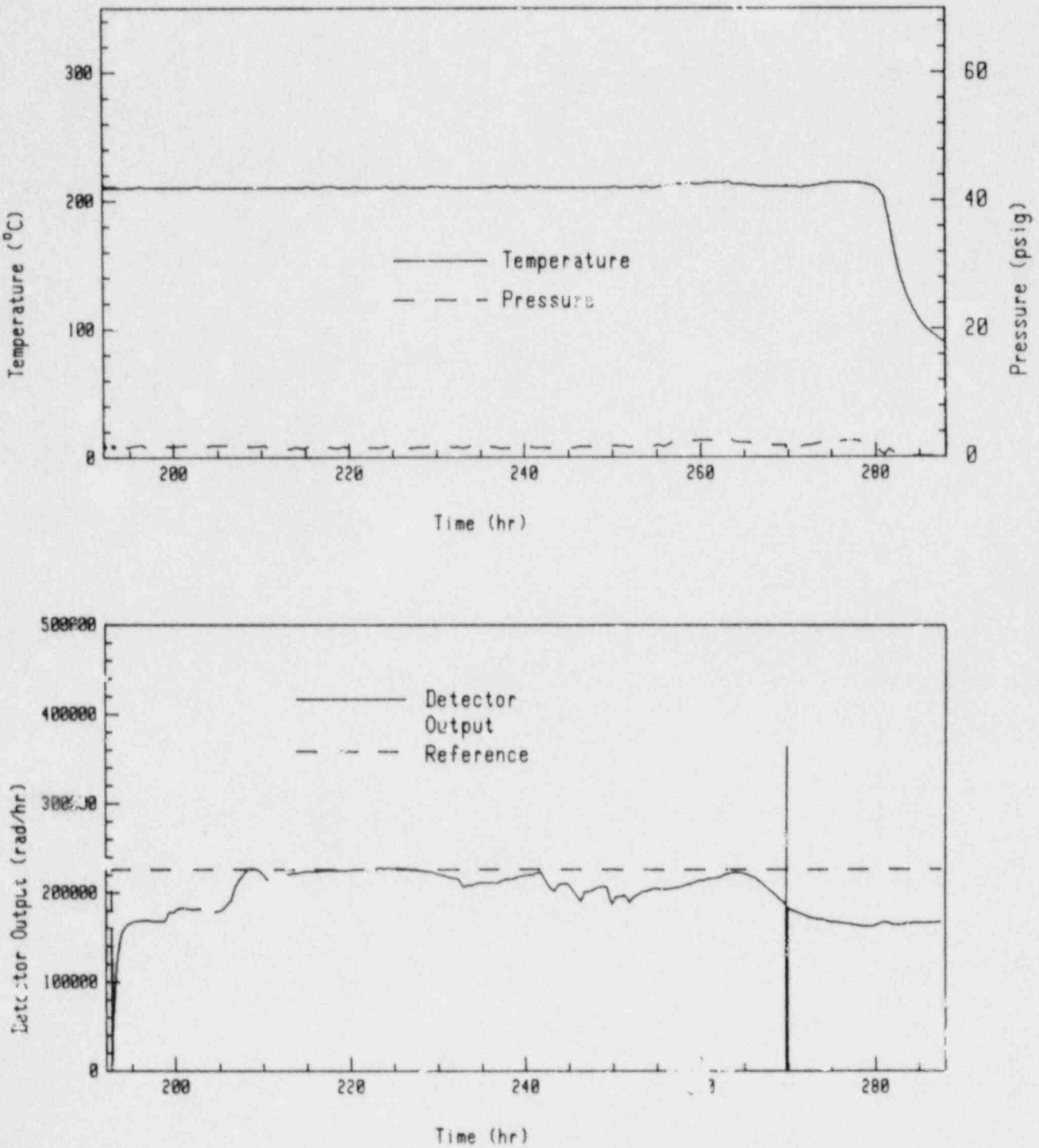

Figure 10e. Chamber Pressure and Temperature and Detector Output.

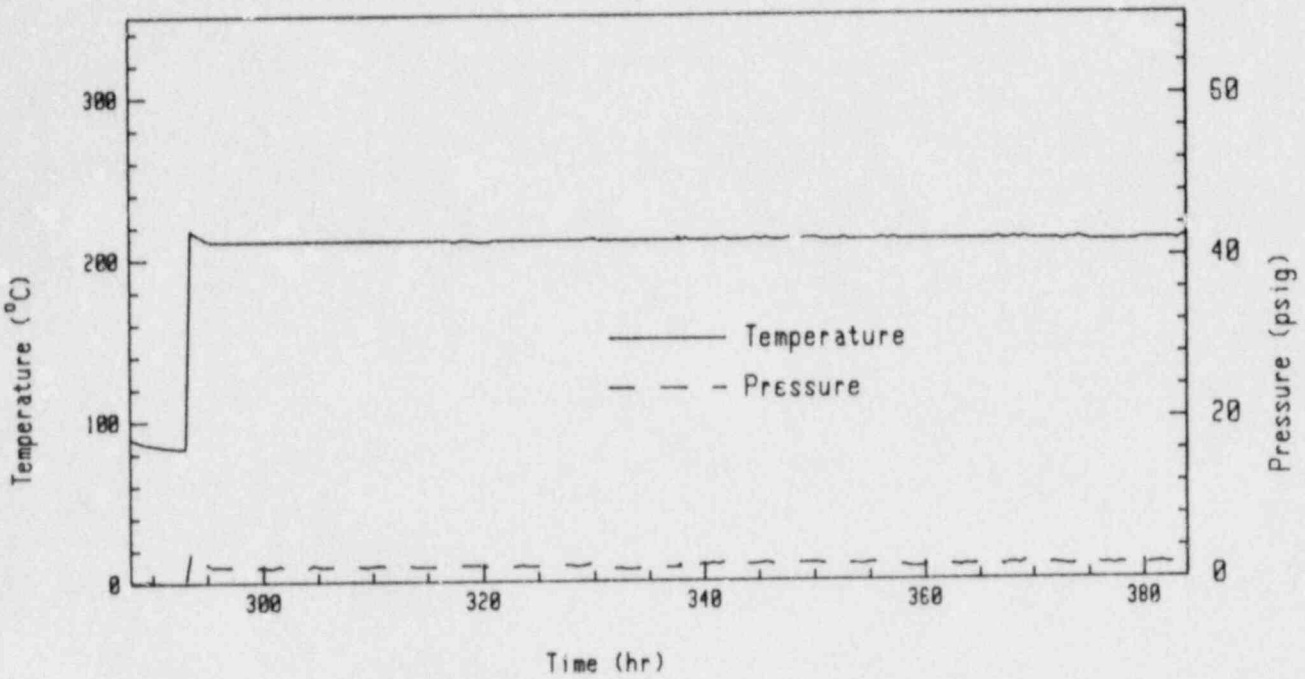

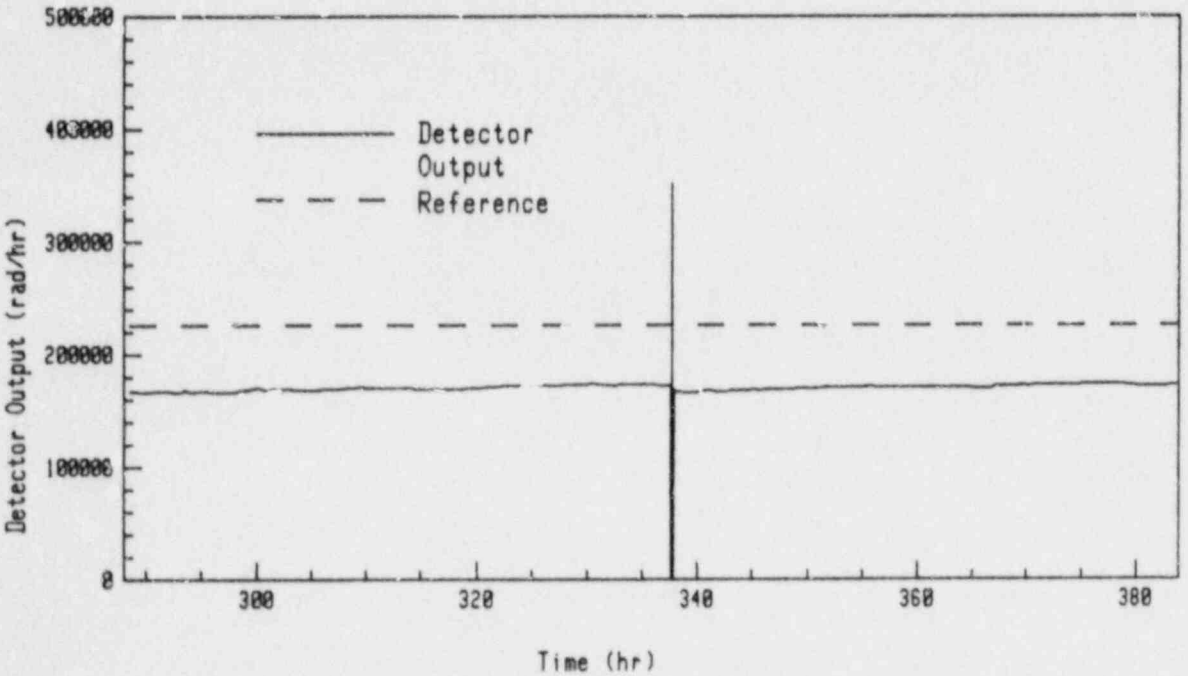

Figure 10. Chamber Pressure and Temperature and Detector Output.

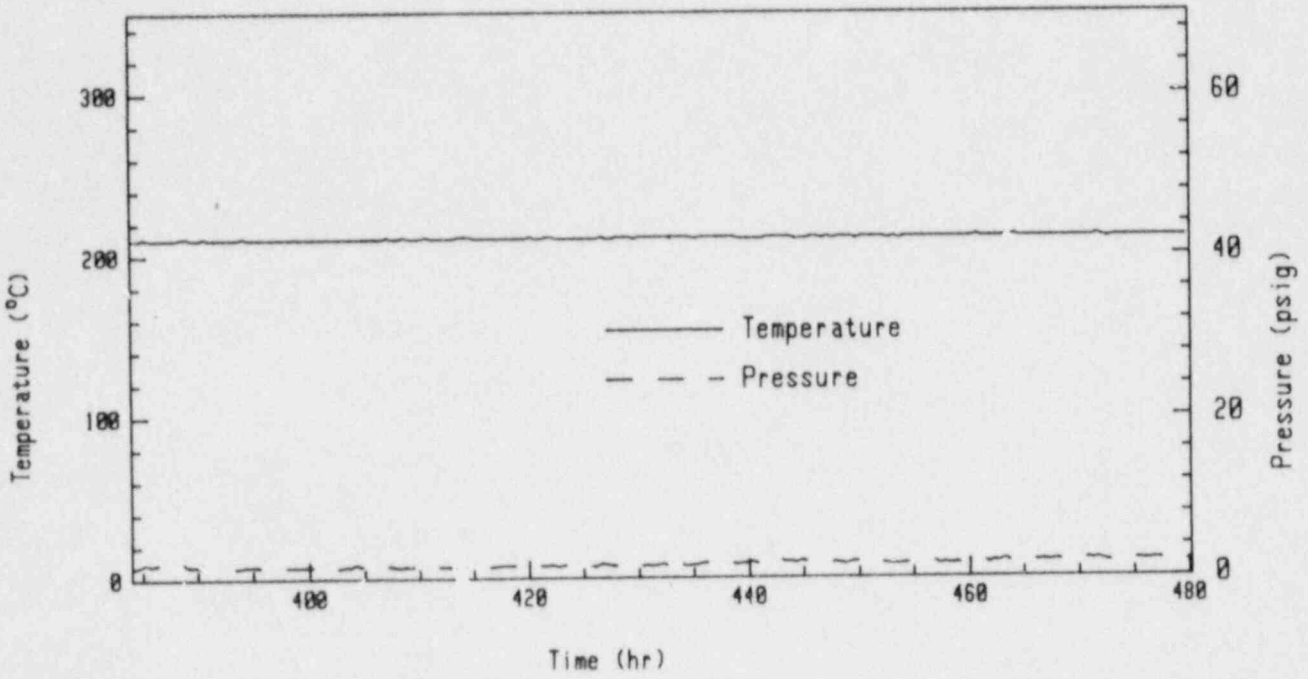

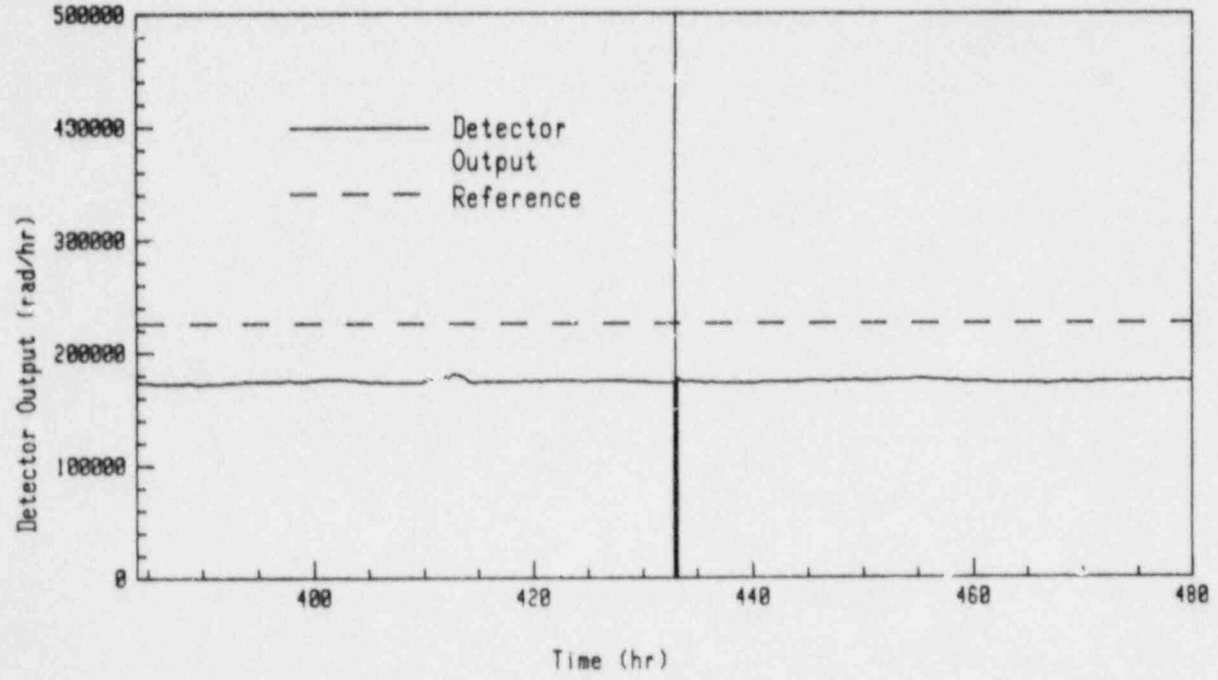

Figure 10g. Chamber Pressure and Temperature and Detector Output.

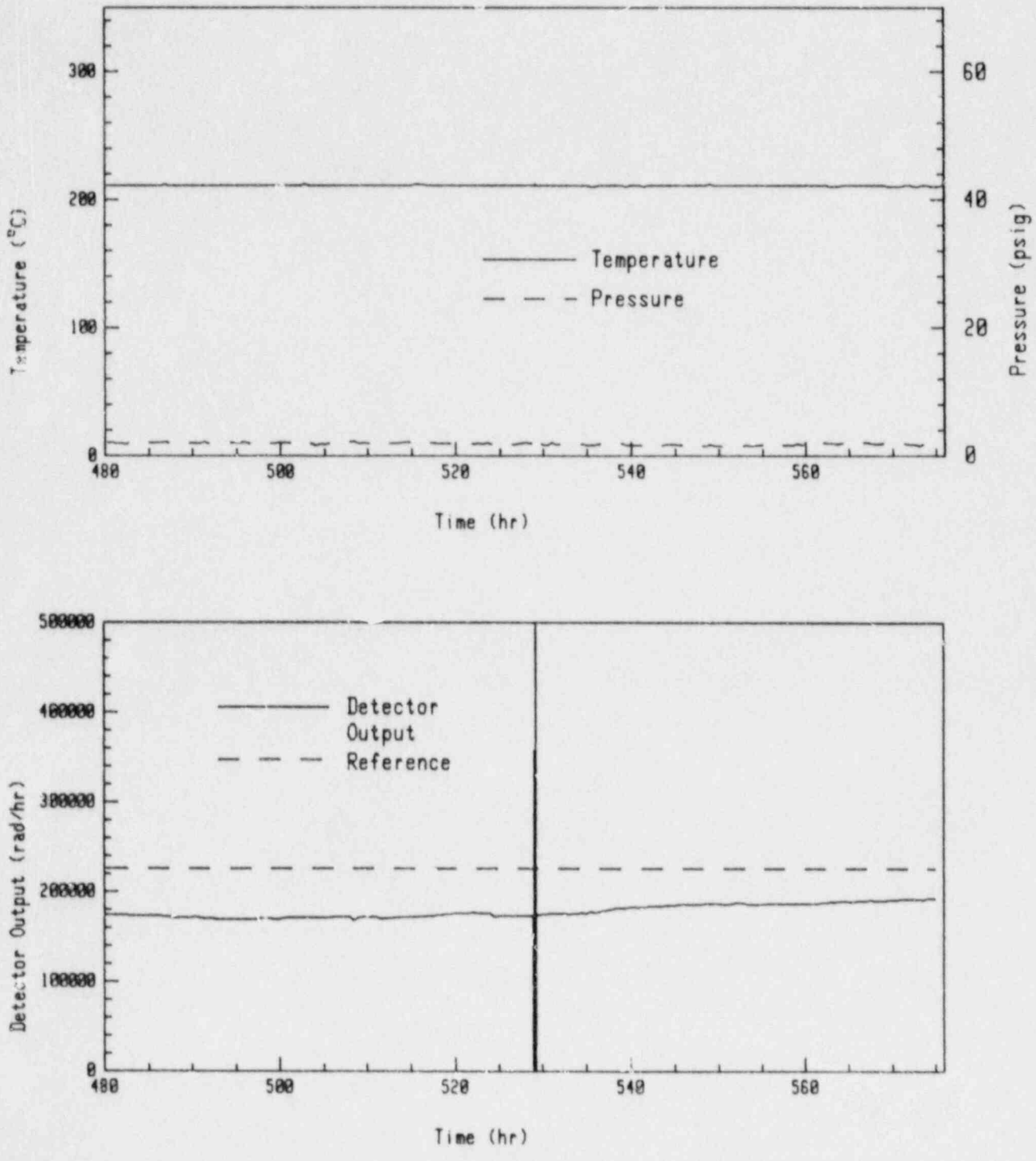

Figure 10h. Chamber Pressure and Temperature and Detector Output.

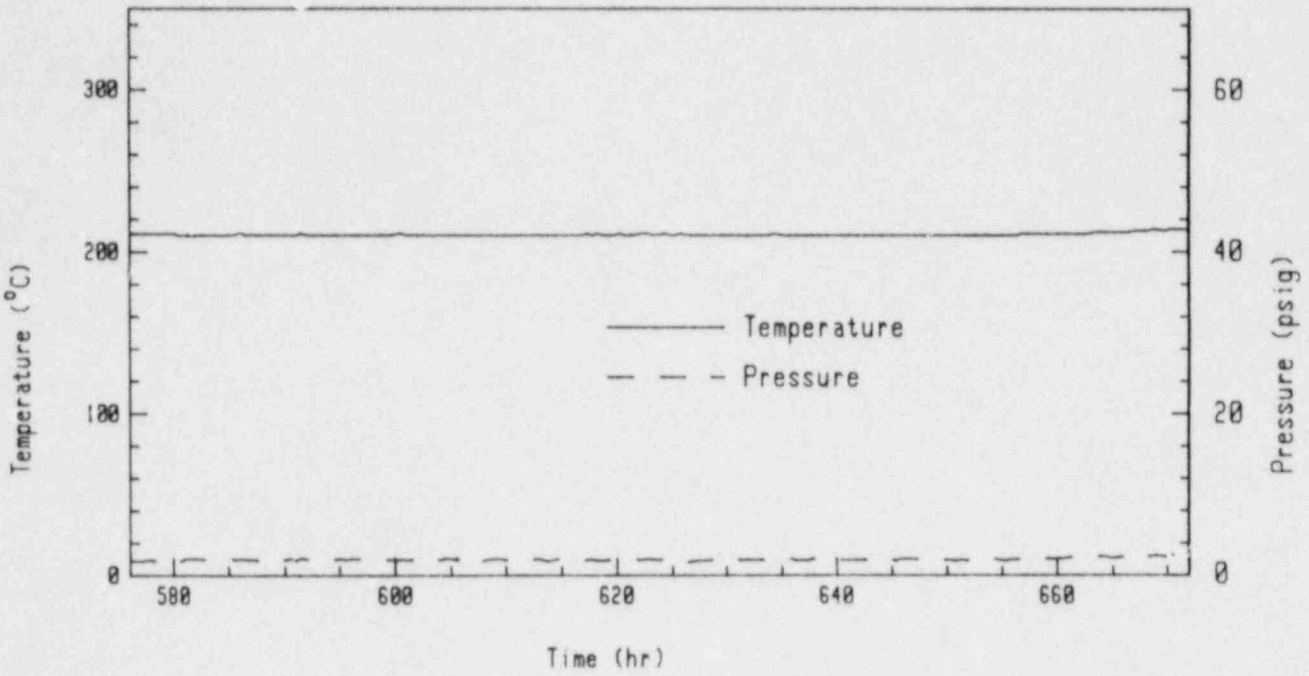

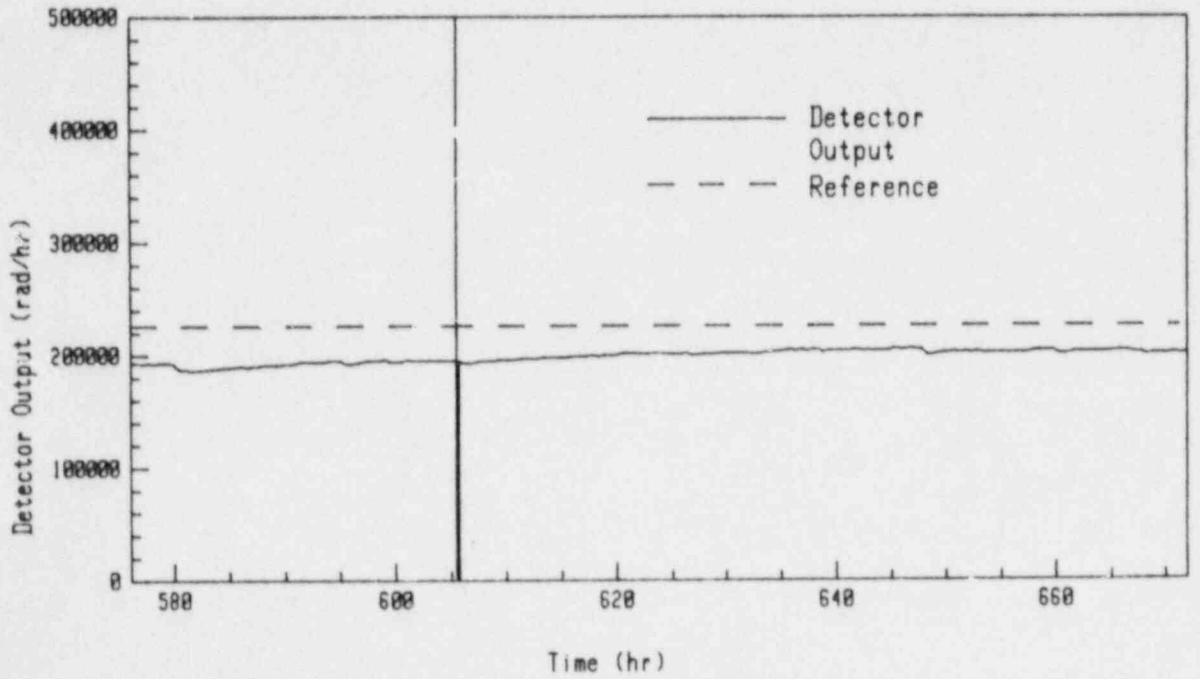

Figure 10i. Chamber Pressure and Temperature and Detector Output.

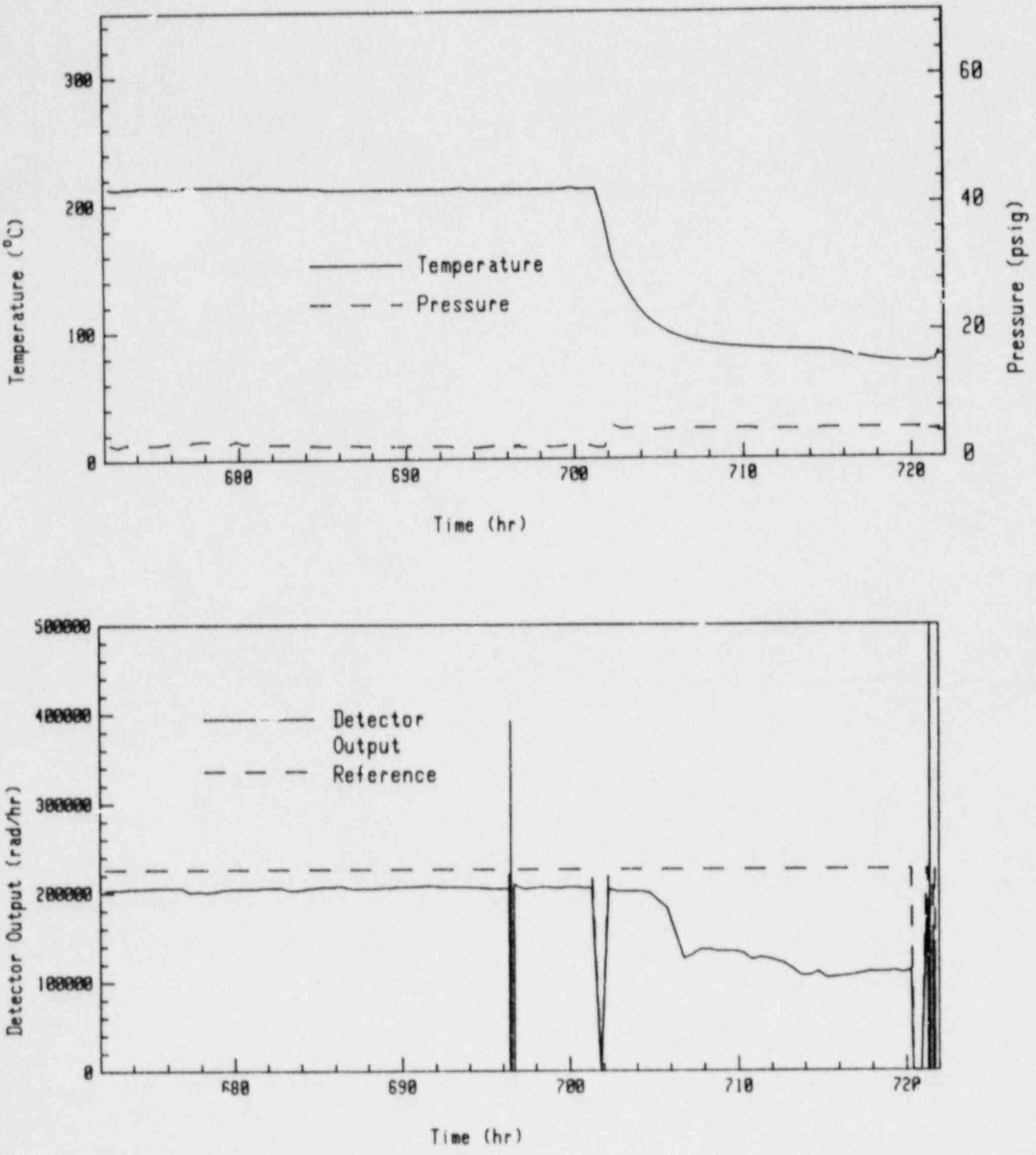

Figure 10j. Chamber Pressure and Temperature and Detector Output.

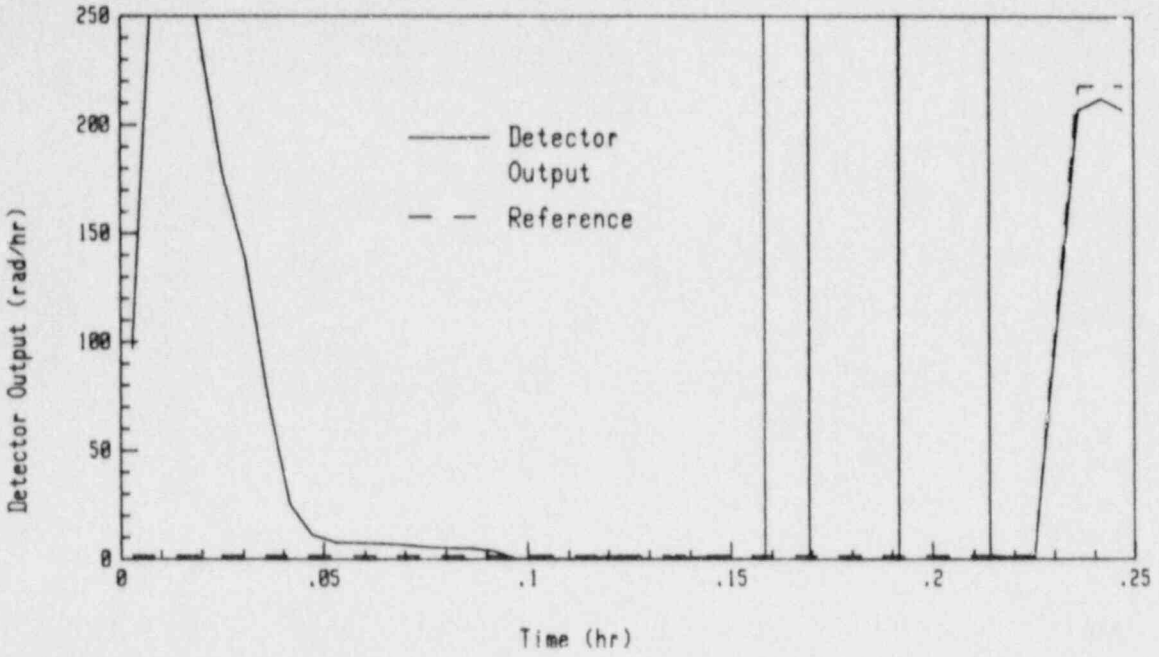

Figure 11. Detector Output at Beginning of Test.

elevator still up (dose rate about 218 rad/hr). A calibration check (#2) was then made; the results are given in Table 4. The test was continued, and more variations in the detector signal were evident around 56 hours (Figure 12c). The calibration procedure was repeated at about 72 hours (#3) with the same results as #2. Again, the accuracy appeared to be decreasing somewhat, but was still within a factor of two at the higher levels. Unfortunately, the HIACA did not have the capability to provide dose rates between 218 rad/hr (elevator up) and 2×10^5 rad/hr (one rod group up), so we were unable to establish thresholds at which the signal disappeared.

About 75 hours into the test, the strip chart recorded an aberration in the detector signal (Figure 12d), and we ran a calibration check (#4 on Table 4) an hour later. We then decided to check the insulation resistance (IR) of the cables leading into the detector (see section 3.3.2.2); the results are given in Table 5 (#1). The signal cable showed reduced IR, while the high voltage cable showed relatively high IR (perhaps because of the high voltage keeping moisture out).

At 161 hours, the strip chart recorded another blip (Figure 12e). A calibration run (#7) was made at 168 hours. For the next 24 hours, the signal varied somewhat, increasing from 1.7×10^5 to 2.0×10^5 rad/hr in 12 hours, holding for 3 hours, then decreasing to 4.7×10^4 rad/hr in 9 hours, at which point (192 hours into the test) calibration #8 was done.

Following an IR check at 193 hours, the detector signal was very slow to respond when a nominal dose rate of 2.26×10^5 rad/hr was applied. The readout slowly increased from about

Table 4. Calibration Data.

#1 Original Calibration	#2 53 hr.		#3 71 hr.	#4 74 hr.	#5 75 hr.	#6 102 hr.	#7 168 hr.	#8 192 hr.
T=Ambient	T=122°C		T=123°C	T=123°C	T=123°C	T=100°C	T=100°C	T=99°C
1.5	0 -100%	*	0 -100%				0 -100%	
218	0 -100%		0 -100%	0 -100%	0 -100%	0 -100%	0 -100%	0 -100%
2.03E+05	1.55E+05 -23.6%		1.94E+05 -4.4%	7.46E+04 -63.3%	3.00E+04 -85.2%	1.97E+05 -3.0%	1.44E+05 -29.1%	2.44E+04 -88.0%
4.11E+05	3.69E+05 -10.2%		3.90E+05 -5.1%	3.03E+05 -26.3%	2.28E+05 -44.5%	4.17E+05 1.5%	4.22E+05 2.7%	2.05E+05 -50.1%
1.21E+06	****		1.18E+06 -2.5%	1.08E+06 -10.7%	9.56E+05 -21.0%	1.23E+06 1.7%	1.11E+06 -8.3%	8.87E+05 -26.7%
2.00E+06	2.02E+06 1.0%		1.97E+06 -1.5%	1.85E+06 -7.5%	1.74E+06 -13%	2.05E+06 2.5%	1.86E+06 -7.0%	1.58E+06 -21.0%
2.77E+06	2.79E+06 0.7%		2.71E+06 -2.2%	2.57E+06 -7.2%	2.44E+06 -11.9%	2.86E+06 3.2%	2.59E+06 -6.5%	2.24E+06 -19.1%
3.49E+06	3.52E+06 0.9%		3.45E+06 -1.1%	3.23E+06 -7.4%	3.09E+06 -11.5%	3.58E+06 2.6%	3.33E+06 -4.6%	2.87E+06 -17.8%
3.71E+06	3.75E+06 1.1%		3.65E+06 -1.6%	3.46E+06 -6.7%	3.29E+06 -11.3%	3.85E+06 3.8%	3.54E+06 -4.6%	3.04E+06 -18.1%
3.89E+06	3.95E+06 1.5%		3.87E+06 -0.5%	3.60E+06 -7.5%	3.48E+06 -10.5%	4.05E+06 4.1%	3.73E+06 -4.1%	3.23E+06 -17.0%

* Values in the tables are arranged as follows:

Indicated dose rate (rad/hr) from detector output.
Error compared to the baseline value given in the first column.

Table 4. Calibration Data. (cont.)

#1 Original Calibration	#9 193 hr.	#10 338 hr.	#11 433 hr.	#12 529 hr.	#13 606 hr.	#14 697 hr.	#15 * Post-Test
T=Ambient	T=99°C	T=100°C	T=99°C	T=99°C	T=99°C	T=99°C	T=Ambient
1.5		0 -100%	0 -100%			0 -100%	0 -100%
218	0 -100%	0 -100%	0 -100%		0 -100%	0 -100%	0 -100%
2.03E+05	1.59E+05 -21.7%	1.47E+05 -27.6%	1.57E+05 -22.7%	1.55E+05 -23.6%	1.73E+05 -14.8%	1.87E+05 -7.9%	1.28E+05 -36.9%
4.11E+05	3.6 E+05 -11.7%	3.52E+05 -14.4%	3.60E+05 -12.4%	3.58E+05 -12.9%	3.73E+05 -9.2%	3.92E+05 -4.6%	3.27E+05 -20.4%
1.21E+06	1.14E+06 -5.8%	1.13E+06 -6.6%	1.13E+06 -6.6%	1.13E+06 -6.6%	1.14E+06 -5.8%	1.17E+06 -3.3%	1.09E+06 -9.9%
2.00E+06	1.92E+06 -4.0%	1.90E+06 -5.0%	1.90E+06 -5.0%	1.90E+06 -5.0%	1.92E+06 -4.0%	1.96E+06 -2.0%	1.86E+06 -7.0%
2.77E+06	2.67E+06 -3.6%	2.64E+06 -4.7%	2.36E+06 -14.8%	2.64E+06 -4.7%	2.66E+06 -4.0%	2.71E+06 -2.2%	2.58E+06 -6.9%
3.49E+06	3.37E+06 -3.4%	3.35E+06 -4.0%	3.34E+06 -4.3%	3.34E+06 -4.3%	3.37E+06 -3.4%	3.44E+06 -1.4%	3.28E+06 -6.0%
3.71E+06	3.58E+06 -3.5%	3.55E+06 -4.3%	3.55E+06 -4.3%	3.54E+06 -4.6%	3.57E+06 -3.8%	3.64E+06 -1.9%	3.49E+06 -5.9%
3.89E+06	3.79E+06 -2.6%	3.74E+06 -3.9%	3.68E+06 -5.4%	3.73E+06 -4.1%	3.77E+06 -3.1%	3.84E+06 -1.3%	3.60E+06 -7.5%

* The post test calibration was run after about 20 hours of exposure to ambient air. Note also that Co-60 decays by approximately 1% over a 30 day period, accounting for a small portion of the observed dose rate decreases.

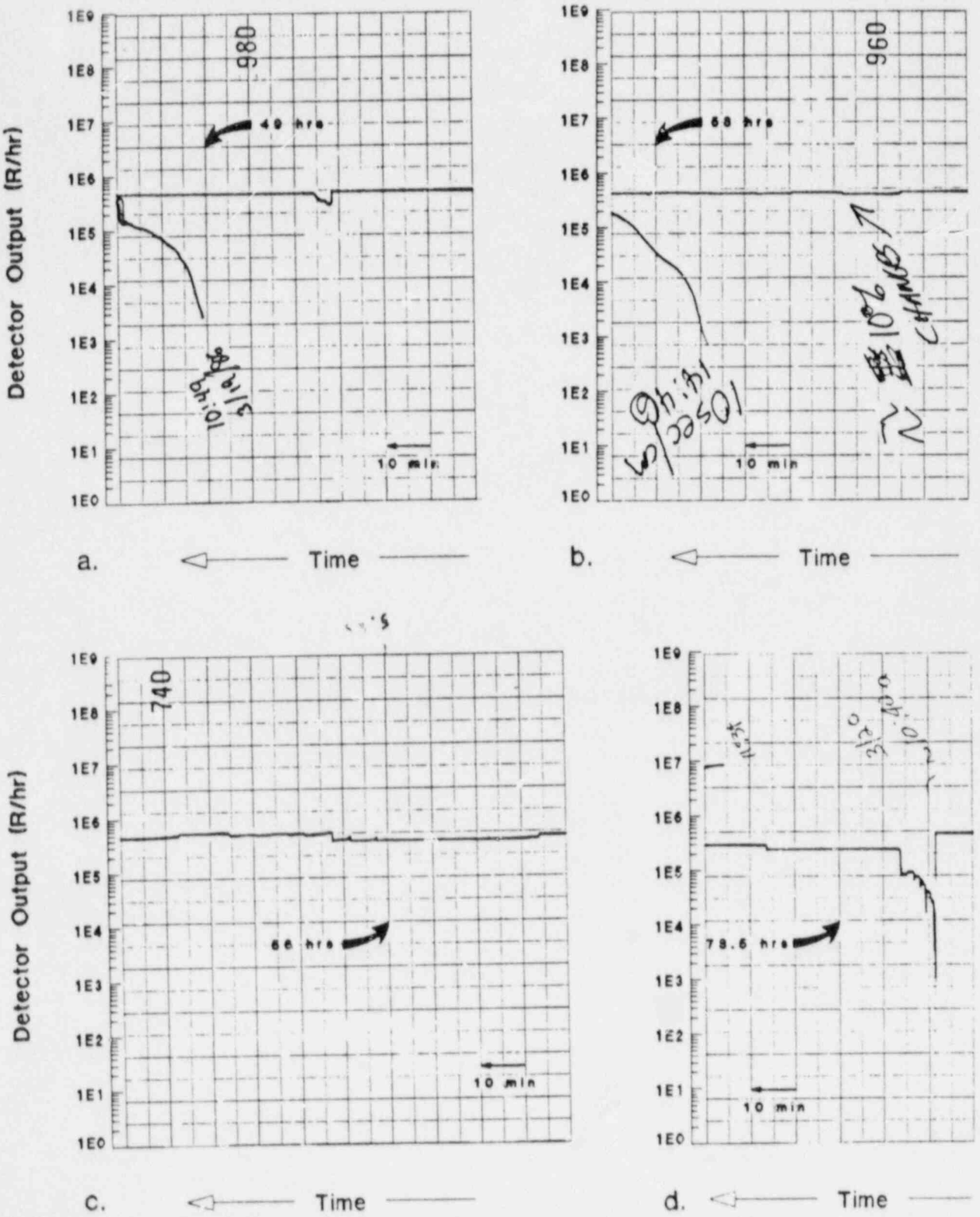

Figure 12. Strip Chart Record of Detector Output.

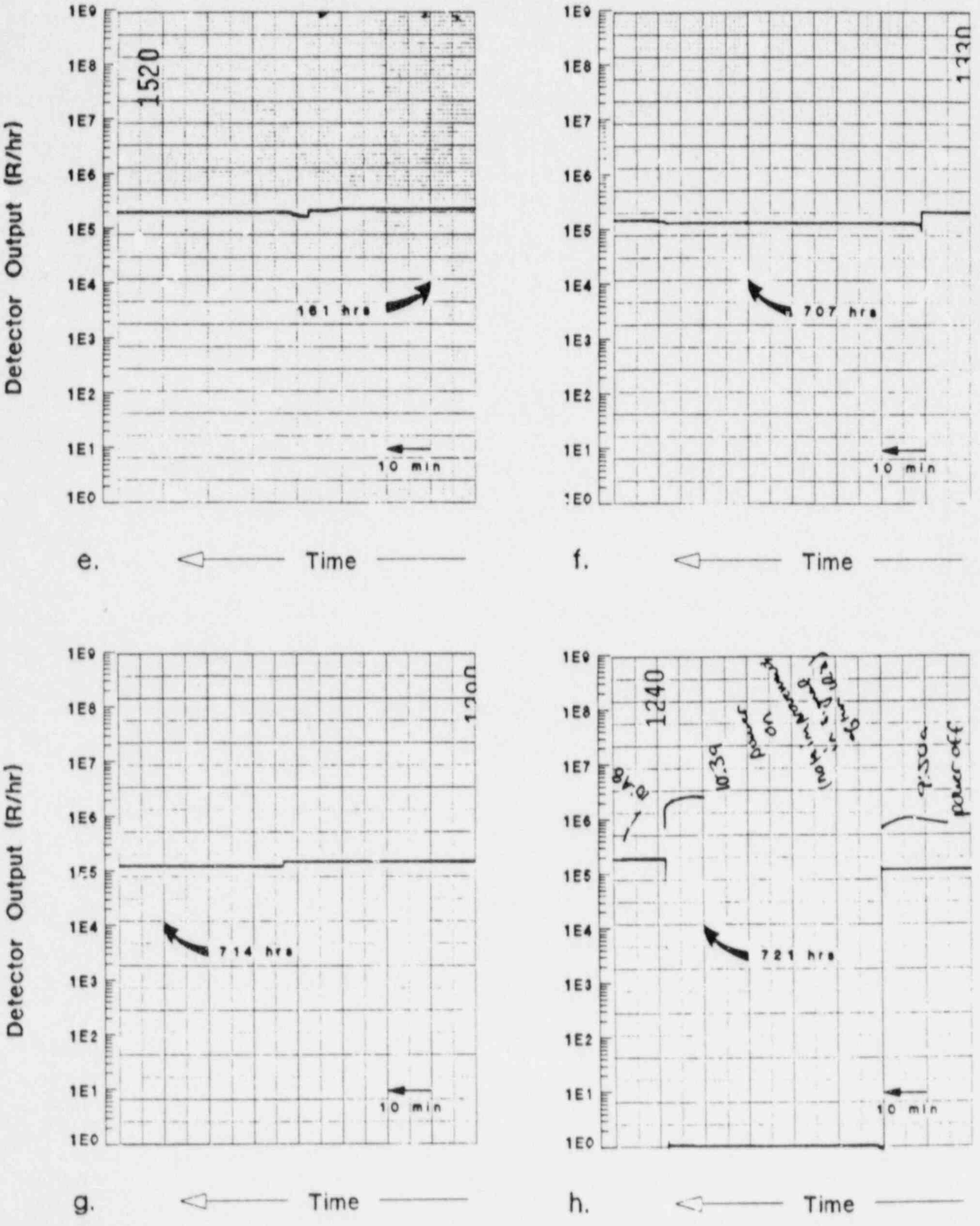

Figure 12 (continued).

Table 5. Cable Insulation Resistance During Test.

a. Signal Cable

Time into Test (hr)	Insulation Resistance (Ω) * at 50 V	100 V	500 V	1000 V
74	9.5E+05	3.3E+05	**	***
192	1.1E+06	2.2E+06	1-2E+07#	***
720	2.4E+05#	3.5E+05#	4.5E+06#	3.5E+06# 6.0E+06## 6.0E+06###
3 wk after test end	7.5E+05	1.1E+06	1.5E+07	6.0E+07

b. High-Voltage Cable

Time into Test (hr)	Insulation Resistance (Ω) * at 50 V	100 V	500 V	1000 V
74	6.5E+10	5.0E+10	1.1E+10	***
192	6.8E+09	1.2E+10	2.8E+10	***
720	9.0E+06	1.7E+07	8.0E+07	8.0E+07
3 wk after test end	5.0E+11	2.0E+12	5.0E+12	5.0E+10

* All measurements taken at one minute unless otherwise noted
** Reading varied excessively and was not recorded
*** Measurement not made at this voltage
\# Reading was unsteady
Measurement made at 6 minutes, reading more steady
Measurement at 11 minutes, after reading was stable

1.2×10^4 rad/hr to 1.15×10^5 rad/hr (within a factor of two of the nominal value) in 30 minutes, followed by essentially complete recovery (at this dose rate) about 14 hours later.

For the remainder of the 30-day steam exposure (dose rate at nominally 2.26×10^5 except during calibrations), the system gave low readings, but within a factor of two. The error varied somewhat, but was typically between about -5 and -25%.

At 702 hours, the radiation source was removed and the detector signal was lost. The steam system was then shut down and an air line was connected to the chamber to dry it out. The radiation was again applied at nominally 2.26×10^5 rad/hr. During the next 18 hours, the detector signal accuracy worsened in the negative direction and was almost precisely a factor of two low when it stabilized. The decreases in accuracy were due mostly to two discrete steps, rather than gradual degradation (Figures 12f and 12g).

At 721 hours, we again measured the IR of the connecting cables with the results shown in Table 5. The results were

low, considering the ambient temperature and that the chamber had been drying out for almost a day. We noted significant fluctuations during the measurements, but they would eventually stabilize, indicating that moisture was still present in the cables/connections and was probably being driven off by the applied voltage. When power was restored to the detector, the accuracy of the system had improved significantly -- the output went from 1.1×10^5 rad/hr before the IR checks to 1.7×10^5 rad/hr immediately after (Figure 12h). At this point, a final calibration check was run with the results given in Table 4, calibration #15.

Three weeks later, the detector was checked for the low-level keep-alive signal, but it had not returned. We then repeated IR measurements on the cables and found they had improved significantly as shown in Table 5. We observed that the readings were steady, unlike the readings taken at 721 hours. At this point, we removed the detector from the chamber to conduct post-test analysis. We noted that the jacket of the signal cable had a small split where the cable entered the sealed conduit (see section 5).

We began the post-test assessment of the detector about two months after removing it from the chamber. At this point, we discovered that the keep-alive signal had returned. The next section discusses our findings from the subsequent examinations and measurements that we made on the detector and readout module.

5.0 Analysis of Test Results

5.1 Data from Bench Tests

The major anomaly noted during the test was the loss of the detector signal at low dose rates at different points during the test. The keep-alive signal loss occurred soon after introduction of steam into the test chamber, followed by return of the signal after several minutes when we increased the dose rate to 218 rad/hr by raising the elevator. The keep-alive signal was then detectable for the duration of the superheated steam exposure and for some time during the saturated steam exposure (based on three checks as stated in Sec. 4.0 above). It disappeared again some time between 30 and 53 hours into the test (saturated steam conditions). At 53 hours, neither the keep-alive signal nor the 218 rad/hr nominal dose rate would produce a reading from the detector.

Several observations during the test led us to believe that the signal loss had been caused by low-level leakage currents in the signal cable: (a) the signal was lost during the time that moisture was most prevalent in the chamber, i.e., during saturated steam conditions and in the early part of the superheat conditions when moisture would have been condensing on the relatively cooler components in the chamber (higher moisture conditions are typically associated with increased leakage currents); (b) insulation resistance measurements made on the signal cable indicated decreased resistance values; (c) we reasoned that leakage currents in the circuit would cause a path for the detector signal to leak to the circuit common and hence never be seen at the detector readout module; and (d) the small split in the jacket could have provided a convenient entry point for moisture, although we would have expected moisture intrusion through the polymeric cable jacket anyway.

We conducted post-test analyses in an attempt to verify the cause of the loss of the keep-alive signal and determine experimentally the magnitude of the readout module error at various input current levels and various cable insulation resistances. We used a picoamp current source to simulate the detector signal, various resistors between the coaxial center conductor and shield to simulate lowered IR values, and a voltmeter to monitor the readout module output. The voltmeter was used for indication only and was not calibrated. (Lack of calibration is unimportant for three reasons: (a) the primary importance of the readings is how they compare in a relative sense to baseline readings, (b) the voltmeter readings corresponded very well to the readings on the readout module meter, but were much easier to read and record, and (c) the calibration curve for the detector, based on the voltmeter readings, was very nearly linear.)

The results of this experiment are shown in Table 6. Because this experiment was looking only for trends and causes,

Table 6. Experimentally Determined Outputs of the Readout Module for Various Insulation Resistances and Input Currents.

Input Current (A)	Simulated Dose Rate (rad/hr)	Leakage Resistance: Infinite	20 MΩ	10 MΩ	1.1 MΩ	105 kΩ	10 kΩ	Short
10E-11	10E0	0.000 *			0.251	0.375	0.449	0.471
		1.0			1.1E2	1.1E3	4.5E3	6.8E3
					+1.1E4%	+1.1E5%	+4.5E5%	+6.8E5%
10E-10	10E1	0.120	0.147	0.164	0.257			0.471
		9.6	16	22	1.2E2			6.8E3
			+67%	+129%	+1.2E3%			+7.1E4%
10E-9	10E2	0.244	0.248	0.251	0.285			0.471
		97	1.1E2	1.1E2	2.1E2			6.8E3
			+13%	+13%	+116%			+6.9E3%
10E-8	10E3	0.369	0.369	0.370	0.374			0.471
		1.0E3	1.0E3	1.0E3	1.1E3			6.8E3
			0%	0%	+10%			+580%
10E-7	10E4	0.496			0.496	0.493	0.483	0.471
		1.1E4			1.1E4	1.0E4	8.6E3	6.9E3
					0%	-9%	-22%	-38%
10E-6	10E5	0.619				0.610	0.567	0.471
		1.1E5				9.2E4	4.1E4	6.8E3
						-16%	-63%	-94%
10E-5	10E6	0.734			0.733	0.726	0.682	0.471
		9.4E5			9.2E5	8.1E5	3.5E5	6.8E3
					-2%	-14%		
10E-4	10E7	0.858			0.858	0.851	0.806	0.471
		(9.6E6)			(9.6E6)	(8.4E6)	(3.6E6)	(6.8E3)
0.0	**	***	0.087	0.125	0.245	0.368	0.450	0.471
			(5.2)	(11)	(99)	(9.9E2)	(4.6E3)	(6.8E3)

* Values in the table are arranged as follows:
a) Voltage measured at the readout output (0-1 V)
b) Corresponding radiation dose rate from calibration curve of best fit semilog line of voltage vs. simulated dose rate: DR_C=1.0122*exp(18.72*V) where V is voltage and DR_C is the calculated dose rate. (Correlation coefficient=0.99984.)
c) Percent error calculated as the ratio of the calculated dose rate with the given leakage resistor minus the calculated dose rate with infinite leakage resistance to the calculated dose rate with infinite leakage resistance times 100%.

** Simulates a loss of the detector signal. Percent error meaningless.

*** Detector went into fault mode signalling loss of keep-alive signal.

we did not make measurements at all values of detector current and insulation resistance. Table 6 shows that, as expected, the errors at the low end of the range have the most severe accuracy degradation. However, the error at the low end of the range was not in the direction we expected (i.e. had the opposite sign), nor in the direction we had observed during the steam exposure (loss of signal). At the high end of the range, the error was in the expected direction with less severe accuracy loss than at the lower end of the range.

Because of the unexpected results, we decided to submerge the detector, cables, and connections to see how the detector keep-alive signal would respond. We found that the signal drifted upward while the assembly was submerged overnight. This observation is consistent with a decreased IR of the signal cable based on our observations in Table 6; however, we were unable to cause the signal to go off-scale at the low end by inserting any type of leakage resistance in the signal cable. The submergence test also failed to cause the signal to go off-scale at the low end.

We also did tests with resistors between the center conductor and the shield of the high voltage cable to assess the impact of degraded insulation resistance on the high voltage lead. We found that with no shunt resistance, the high voltage supply produced a nominal voltage of 875 V. The voltage degraded to about 800 V when we added a 1 MΩ resistor across the high voltage cable, to about 650 V when we added 422 kΩ, to about 460 V when we added 211 kΩ, and to about 300 V when we added 105 kΩ. The detector keep-alive signal decreased with lowered resistances, and the operation indicator light went off with 211 kΩ across the high-voltage cable. We did not assess accuracy over the entire instrument range under degraded high voltages, but we feel that a criterion of 1 MΩ for the parallel combination of insulation resistances of the cable, penetration, connections, etc., would be a reasonable specification for the high-voltage side interconnection.

5.2 Analysis of Data from Bench Test

We investigated the cause of the unexpected response to insulation resistance effects by examining the circuit schematic for the detector. As a result, we believe that knowledge of the offset voltage characteristics of the readout module's input operational amplifier is critical to assessing the loss of accuracy of the readout module caused by insulation resistance effects. To illustrate the point, an operational amplifier circuit is shown in Figure 13. In this circuit, under ideal conditions, all of the input current is diverted around the input amplifier and through select feedback elements. Under these conditions, the negative terminal of the input amplifier acts as a "virtual" ground, i.e., the voltage across the amplifier inputs, V_1, is very nearly at ground potential. The output voltage of the amplifier must be

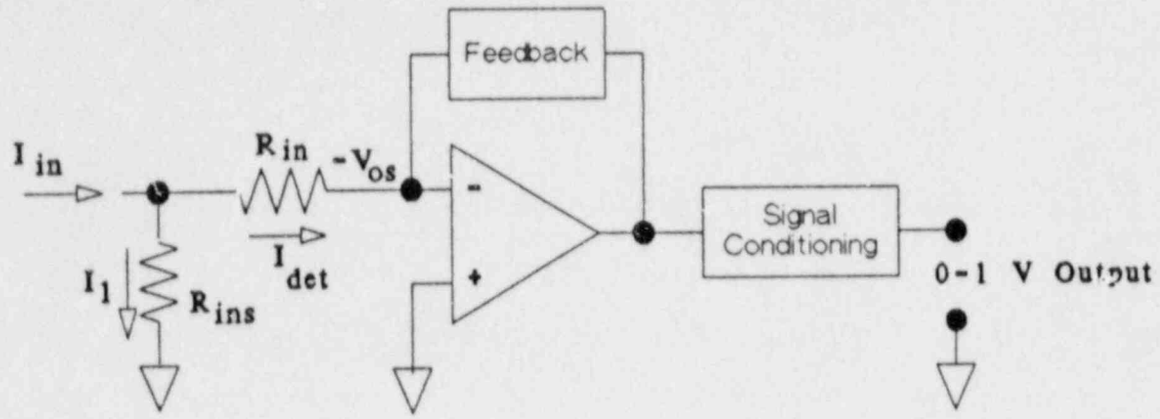

Figure 13. Block Diagram of Operational Amplifier Circuit.

$V_{out} = -A*V_1$, where A is the open loop amplifier gain. (The amplifier gain could vary over a wide range, but a typical value might be around 2×10^5.) The actual voltage V_1 is "adjusted" by the feedback elements so that the desired closed loop properties of the output voltage are achieved. The amplifier voltage output range is approximately 12 V to 0 V, decreasing in proportion to the logarithm of the input current. With no input signal, the amplifier output voltage is about 12 V, while with an input signal of 10 mA, the amplifier output voltage is about 0 V. The voltage at the 0-1 V output of the readout module is scaled and offset from the amplifier output so that an input current to the readout module of 10^{-11} A gives an output of 0 V and an input of 1 mA gives an output of 1.0 V. The voltage measurements shown in Table 6 are taken from the 0-1 V output. As an example of the voltage at V_1, consider the above open loop amplifier gain and an output voltage of 5.0 V. The resulting voltage V_1 is easily calculated as 0.025 mV (indeed a "virtual" ground). Any input offset voltage is automatically compensated for by the feedback elements since the input current is completely controlling the feedback characteristics. This compensation is manifested as the above calculated voltage "floating" on the input offset voltage. In the above example, if the input offset voltage were +1.5 mV, the actual voltage V_1 would be -1.5 mV + 0.025 mV = -1.5 mV, or essentially just the offset voltage (negative offset voltage since V_1 is located at the negative amplifier input). In fact, regardless of the amplifier output over a wide range, V_1 remains at approximately the negative of the offset voltage as long as the amplifier open loop gain is high.

Next, consider the effect of finite insulation resistance and nonzero input offset voltage on the circuit of Figure 13. Finite insulation resistance will exist from cables, connectors, penetrations, or other interconnecting devices. The voltage V_1 is nearly at ground potential (-1.5 mV for the case described above). Based on a center conductor resistance

of 20 ohms, it can easily be shown that the voltage along the center conductor of the coaxial cable is essentially uniform along the length of the cable at any given detector current. The following analysis demonstrates how the errors shown in Table 6 may be predicted analytically if the input offset voltage is known. As discussed above, V_1 is essentially constant over much of the range of detector currents if the amplifier gain is high. Thus the input offset voltage can be easily measured as the voltage V_1 with a small input current. For our detector, the input offset voltage was measured as about 1.5 mV (V_1 = -1.5 mV). The measurement was checked at several input currents from about 10^{-8} A to 10^{-4} A with only a slight change in V_1, indicating a high enough amplifier gain to keep V_1 approximately constant over that range. Referring to Figure 13 and summing currents at node 1 gives:

$$I_1 + I_{det} = I_{in} \qquad (1)$$

With $I_1 = V_1 / R_{ins}$, (1) becomes:

$$\frac{V_1}{R_{ins}} + I_{det} = I_{in} \qquad (2)$$

With $I_{det} = (V_1 + V_{os}) / R_{in}$, where V_{os} is the amplifier input offset voltage, (2) becomes:

$$\frac{V_1}{R_{ins}} + \frac{V_1 + V_{os}}{R_{in}} = I_{in} \qquad (3)$$

Solving (3) for V_1 gives:

$$V_1 = \left(\frac{R_{in} R_{ins}}{R_{in} + R_{ins}} \right) \left(I_{in} - \frac{V_{os}}{R_{in}} \right) \qquad (4)$$

Finally, using (4) in (2) and rearranging gives:

$$I_{det} = I_{in} \left(\frac{R_{ins}}{R_{in} + R_{ins}} \right) + \frac{V_{os}}{R_{in} + R_{ins}} \qquad (5)$$

Equation 5 gives an expression for the current actually measured by the readout module for a given offset voltage and a given insulation resistance between the center conductor and shield of the coaxial cable.

To illustrate how well equation 5 works, we will use the input offset voltage of our readout module's input amplifier (approximately 1.5 mV). As a first case, consider an insulation resistance of 1.1 MΩ and a detector current of 10^{-10} A. The value of R_{in} was verified by measurement to be 20 kΩ. Substituting into equation 5 gives an input current

of 1.46×10^{-9} A which corresponds to a dose rate of 146 rad/hr. Using the equation from the footnotes of Table 6 gives a readout module output voltage of 0.266 V, which compares extremely well to the measured value of 0.257 V given in Table 6. As a second example consider a higher detector current of 10^{-5} A with an insulation resistance of 10^4 Ω. We recognize that this tends to be a low value for coaxial cable in a steam environment, but we use it here for illustration purposes to get a large enough error so that equation 5 can be meaningfully verified. For this second case, equation 5 gives an input current of 3.33×10^{-4} A. This corresponds to a dose rate of 3.33×10^5 rad/hr and a readout module voltage output of 0.679 V, which compares very favorably with the measured value of 0.682 V given in Table 6. It should be emphasized that this assessment required the knowledge of the input offset voltage of the readout module input operational amplifier. The offset voltage is a random parameter and might typically be within the range of -3.0 mV to +3.0 mV. Consequently, without knowing the input offset voltage for a given device, neither the magnitude nor even the direction of the error is predictable. However, given the manufacturer's specifications for the input amplifier, bounds can be put on the IR-induced error as a function of the detector current and the interconnection insulation resistance by using equation 5.

Equation 5 can also be used to give a qualitative assessment of the readout module's behavior by considering the two terms of the equation separately. The first term represents the loss of signal generated by leakage of detector current to ground; the factor in parenthesis is always a positive quantity less than 1.0. The second term represents the contribution of the amplifier input offset voltage to the input current and may be either positive or negative. If the input offset voltage is positive (as in our case), it causes additional current to flow into the readout input because V_1 is approximately the negative of the offset voltage and is thus below ground potential, causing current to be drawn from ground. A reverse argument holds for a negative offset voltage, but the result is current drawn from the readout module. In this second case, at low detector currents, the readout module will tend toward going off-scale on the low end (due to both terms). At low detector currents, the second term of equation 5 tends to control readout behavior, while at high detector currents, the first term tends to control the behavior. For any given interconnection insulation resistance, the undesirable effects modelled by equation 5 are much more pronounced for the low detector currents (mainly the second term of equation 5).

At this point, we have a model which appears to accurately predict the effect of interconnection insulation resistance on the readout module's error. This prediction was verified over a range of values for our readout module. We have one

significant problem remaining, that of explaining why in the test the detector signal was lost altogether during periods of high moisture conditions. Obviously, the effect of insulation resistance, which prior to post-test analysis seemed to be the certain explanation, is not the proper explanation. We postulated only one theory which might explain the detector's behavior: galvanic action between two dissimilar materials somewhere in the interconnections to the detector. Theoretically, a voltage induced on the coaxial cable's center conductor which has the effect of reducing the voltage at the readout module input would tend to allow less current to flow into the readout module. At some lower potential which could be positive or negative, the induced voltage at the input would equal the negative of the amplifier offset voltage (-1.5 mV in our case) and would result in no current into the readout module. At even lower potentials, current would be drawn out of the readout module. Any reduced voltage causes the readout module to go in the negative direction, resulting in the eventual loss of detector signal at some level. For our detector, the measured loss of signal occurred at a voltage very near -1.5 mV, confirming the theoretical discussion above. (This observation <u>may</u> provide an additional means of measuring offset voltage by inducing a reduced voltage on the center conductor of the cable until the signal is lost.) In summary, an induced voltage on the center conductor of the cable approximately equal to the input offset voltage could account for the observed loss of detector signal.

The next question is whether a possible galvanic reaction could supply the necessary voltage and power to account for the observed effects. Certainly a voltage of greater than a few mV is possible with almost any galvanic reaction. Based on the observed lack of signal at a dose rate of 218 rad/hr during our test, we might guess that it would still be lost as high as 1000 rad/hr (it did come back at 2×10^5, but we have no data between 218 and 2×10^5 rad/hr because of the discrete steps available from our radiation source). A dose rate of 1000 rad/hr corresponds to a detector current of 10^{-8} A. For our system, a potential galvanic reaction would need to supply about 1.5×10^{-3} V x 10^{-8} A = 1.5×10^{-11} W = 15 pW, which does not seem to be excessive for a galvanic reaction over a fairly small area. However, we can only very tentatively give this explanation since we did not investigate the root cause completely. We did contact the connector manufacturer and found that the connector uses a brass contact with either silver or gold plating and a brass body with silver plating. The coaxial cable uses tin-coated copper for both the center conductor and the shield. Thus, dissimilar metals do exist and could provide the components for a galvanic reaction.

Galvanic action was the only explanation we could postulate that had a reasonable basis to explain the observed behavior of the detector in the test. In any case, for our system, whatever caused the loss of detector signal at the low

end appears to be more important than IR effects, since we saw some significantly degraded IRs without the expected detector response. Unfortunately, the IR effects were what we could reasonably model, while the "other" effects we could not even positively identify, much less quantify. It does appear that IR effects may have accounted for some of the results we observed during the test, such as possibly the degraded accuracy observed at the end of the test. Finally, note that IRs measured during qualification tests (typically measured at 500-1000 V) may not be truly representative of the IR values at the millivolt levels associated with the signal cable at low detector currents. This is especially relevant where small amounts of moisture may contribute to lowered IR and high voltage measurements can drive off the moisture.

As mentioned previously, when we removed the detector from the chamber, we observed a small split in the cable's jacket, which we at first believed contributed to reduced IR. The split was on the signal cable at the potting where it entered the sealed conduit. The split appeared to have been caused by material degradation resulting from exposure to the harsh environment (high temperature, steam, and radiation) coupled with internal stresses due to thermal expansion of the coaxial cable. At the beginning of the test, the cable went straight from the connector to the potting; after the test, the cable had a (longer) curved path from the connector to the potting, clearly indicating that the cable's length had increased. See Appendix A for further discussion of the cable jacket split.

Although the potting and conduit system used in our test does not necessarily represent actual installations, the cable split again raises the question of whether separate component qualification is sufficient to ensure that a complete, installed system is qualified. Specifically, we used what could be considered a "nuclear-qualified" epoxy (since it did in fact perform its intended function), a qualified cable, and a qualified detector, but the system we created by combining these "qualified" components allowed a failure mode to be created (loss of jacket integrity), one which apparently did not show up in any individual component qualifications.

6.0 Conclusions and Recommendations

6.1 Detector Performance

General Atomic's RD-23 high-range radiation detector is designed to operate in a range of 1 rad/hr to 10^8 rad/hr under extreme pressure, temperature, and moisture conditions. We found that the detector had no trouble "surviving" these conditions, and as long as there was a sufficient radiation dose rate, the detector met the accuracy conditions in RG 1.97.[1] However, at "lower" dose rates the detector signal at the readout module became inaccurate or was lost altogether due to the reasons discussed in section 5. Based on the results, we conclude that while the detector "survived" the test conditions, the overall system (detector, cable, connections) did not meet the requirements in RG 1.97 for the lower dose rates only.

Two concerns identified with the detector operation are as follows:

a. At low radiation dose rates, insulation resistance effects of the interconnections may cause detector accuracy to degrade beyond the factor of two allowed by RG 1.97. The magnitude and direction of the observed error were shown to depend on the interconnection insulation resistance, the readout module input amplifier's input offset voltage, and the detector signal level.

b. A second phenomenon, perhaps galvanic action, caused the detector signal to be lost at low levels of detector output. We were unable to hypothesize any mechanism which would explain the observed loss of signal other than galvanic action. We also noted that for our test this phenomenon appeared to obscure insulation resistance effects at low detector currents. Thus, analysis techniques considering only insulation resistance effects to assess detector accuracy may be of somewhat questionable value. It is possible that the split in the cable jacket contributed to the loss of signal by providing an additional path for moisture intrusion into the connector.

Although the potting and conduit system used in our test does not necessarily represent actual installations, the cable split again raises the question of whether separate component qualification is sufficient to ensure that a complete, installed system is qualified. We used "qualified" components, but the system we created by combining these components created a failure mode which apparently did not show up in any individual component qualifications.

6.2 Recommendations for Radiation Monitor Users

Based on the results of this test, we feel that the detector will operate properly under the most severe design-basis accident conditions; that is, when radiation is at a high level during a LOCA. The problems occurred when the radiation dose rate was relatively low, producing only a small signal current from the detector. Thus, we recommend that users of the RD-23 detector assess the results of this test program as it relates to their detector installation. We also recommend that licensees with other types of high-range radiation detectors review their qualification test data to check for similar concerns.

We feel that utilities need to be aware of the following specifics of the observed GA detector response:

a. Readings at levels below about 1000 rad/hr were not reliable during accident conditions.

b. Readings at levels above about 1000 rad/hr under accident conditions were accurate even though the green "operate" light on the readout module went off several times (it did come back on when it was reset by pushing it).

In addition, utilities should be reminded that installations of components and systems qualified by parts may not constitute a qualified system.

6.3 Recommendations for Future Tests

As stated earlier, we do not feel additional tests of the RD-23 detector itself are warranted, as the detector itself appeared to operate satisfactorily. However, it may be advisable to test other types of radiation detectors that could exhibit similar problems. We do think the coaxial cable/connection system merits further attention; perhaps a general investigation of Class 1E coaxial cable and connections exposed to harsh environmants should be undertaken.

7.0 References

1. "Instrumentation for Light-Water-Cooled Nuclear Power Plants to Assess Plant and Environs Conditions During and Following an Accident," Regulatory Guide 1.97 (Washington, D.C., U.S. Nuclear Regulatory Commission, Revision 2, Dec. 1980).

2. "Clarification of TMI Action Plan Requirements," NUREG-0737 (Washington, D.C.: U.S. Nuclear Regulatory Commission, Nov. 1980).

3. Oliver D. T. Lynch Jr. to William S. Farmer, "Modification of FIN-A1051 to Include Instrumentation Required by NUREG-0737, II.F.1(3)" (Washington, D.C.: US Nuclear Regulatory Commission, Nov 27, 1984). Memorandum.

4. Dennis E. Hadlock and Ronald L. Kathren, "Thermal Limitations of Detectors in High-Level Radiation Fields," Health Physics, 43:1, July 1982.

5. Elizabeth H. Richards and John A. Lewin, "Test Plan - Post Accident Monitoring - High-Range Radiation Monitor" (unpublished) (Albuquerque: Sandia National Laboratories, July 12, 1985.)

6. "Specifications for Backfit Digital Radiation Monitoring Systems" (San Diego: GA Technologies E-162-1147, 1983).

7. "High-Range Gamma Radiation Monitoring System -- Operation and Maintenance Manual" (San Diego: GA Technologies E-115-876 Rev. 2, November 1981).

8. "High-Range Containment and Steam Line Radiation Monitors -- Equipment Manual" (San Diego: GA Technologies E-115-1049, November 1981).

9. "Equipment Qualification Data Bank Quarterly Report" (Clearwater, FL: Electric Power Research Institute, April 1984).

10. "IEEE Standard for Qualifying Class 1E Equipment for Nuclear Poewr Generating Stations," IEEE 323-1974 (The Institute of Electrical and Electronic Engineers, 1974).

11. William H. Buckalew and Frank V. Thome, "Radiation Capabilities of the Sandia High Intensity Adjustable Cobalt Array," NUREG/CR-2582, SAND81-2655 (Albuquerque: Sandia National Laboratories, March 1982).

12. J. A. Gieske, et al., "Radionuclide Release Under Specific LWR Accident Conditions," BMI-2104, Vol. 1-6 (Colombus, OH: Battelle Columbus Laboratories, 1984).

APPENDIX A
Discussion of Split in Cable Jacket

Upon removal of the radiation detector from the test chamber, we noted a small split (approximately 3 mm (1/8 in.) long) in the cable jacket where the cable entered the sealed conduit. The split appeared to have been caused by material degradation resulting from exposure to the harsh environment (high temperature, steam, and radiation) coupled with internal stresses due to thermal expansion of the coaxial cable. At the beginning of the test, the cable went straight from the connector to the potting; after the test, the cable had a (longer) curved path from the connector to the potting, clearly indicating that the cable's length had increased.

The split in the jacket may have contributed to allowing moisture to enter the connector via the braid, causing reduced IR as well as a path for galvanic action. However, there are a number of reasons that indicate that even if moisture entered the connector through the crack that moisture would have penetrated to the connector anyway. Moisture is known to permeate polymer materials such as the coaxial cable jacket, and moisture penetration in this fashion takes time. We saw the most significant signal loss somewhere between 30 and 53 hours into the test (first verified at 53 hours). At those times the total dose to the cable was between about 25 and 33 MR. The cable had not been thermally aged prior to the LOCA exposure. The jacket material is an irradiation cross-linked polyethylene and the cable has been tested to 200 MR with thermal aging included. Cross-linked polyethylene in general is considered a very good material for radiation resistance and would be expected to retain good elongation properties after only 30 MR exposure. Additionally, if the major stress causing the crack were the severe transient temperature exposure, we would have expected to see the effects of the crack earlier than 30 hours, since at 30 hours a long term steady-state exposure at 250°F had been going on for 20 hours, and this exposure remained constant to the 53 hour point. Thus, it is very possible that the crack did not appear until later in the test when higher radiation doses were attained. However, we cannot be sure that this was indeed the case. We should also note that signal losses similar to those we observed have been observed in industry tests of radiation monitors, although not in the final "qualified" configuration of the monitors. The signal losses were usually attributed to connection problems. Finally, we note that the errors we observed early in the test were much worse than those reported in industy tests.

If we assumed that the crack was in fact what allowed moisture penetration into the connector, then the following questions would be relevant:

1) The shorter lengths of cables typically used in qualification testing can tend to restrict the amount of

moisture getting to the connector by permeation through cable jackets. How much moisture would have migrated to the connector if a representative length of cable had been connected to the detector?

2) Will jacket integrity be maintained in actual installations which may include different cable products, additional environmental exposures, and various aspects unique to the particular installation?

The answers to these questions are beyond the scope of this study, but perhaps they should be investigated in future studies.

DISTRIBUTION:

U.S. Government Printing Office
Receiving Branch (Attn: NRC Stock)
8610 Cherry Lane
Laurel, MD 20707
330 copies for RV

Ansaldo Impianti
Centro Sperimentale del Boschetto
Corso F.M. Perrone, 118
16161 Genova
ITALY
Attn: C. Bozzolo

Ansaldo Impianti
Via Gabriele D'Annunzio, 113
16121 Genova
ITALY
Attn: S. Grifoni

ASEA-ATOM
Department KRD
Box 53
S-721 04
Vasteras
SWEDEN
Attn: A. Kjellberg

ASEA-ATOM
Department TQD
Box 53
S-721 04
Vasteras
SWEDEN
Attn: T. Granberg

ASEA KABEL AB
P.O. Box 42 108
S-126 12
Stockholm
SWEDEN
Attn: B. Dellby

Atomic Energy of Canada, Ltd.
Instrument and Control Branch
Chalk River Nuclear Laboratories
Chalk River, Ontario K0J 1J0
CANADA
Attn: E. C. Davey

Atomic Energy of Canada, Ltd.
1600 Dorchester Boulevard West
Montreal, Quebec H3H 1P9
CANADA
Attn: S. Nish

Atomic Energy Research
Establishment
Building 47, Division M.D.D.
Harwell, Oxfordshire
OX11 ORA,
ENGLAND
Attn: S. G. Burnay

Bhabha Atomic Research Centre
Health Physics Division
BARC
Bombay-85
INDIA
Attn: S. K. Mehta

British Nuclear Fuels Ltd.
Springfields Works
Salwick, Preston
Lancs
ENGLAND
Attn: W. G. Cunliff, Bldg 334

Brown Boveri Reaktor GMBH
Postfach 5143
D-6800 Mannheim 1
WEST GERMANY
Attn: R. Schemmel

Bundesanstalt fur Materialprufung
Unter den Eichen 87
D-1000 Berlin 45
WEST GERMANY
Attn: K. Wundrich

CEA/CEN-FAR
Departement de Surete Nucleaire
Service d'Analyse Fonctionnelle
B.P. 6
92260 Fontenay-aux-Roses
FRANCE
Attn: M. Le Meur
J. Henry

CERN
Laboratorie 1
CH-1211 Geneve 23
SWITZERLAND
Attn: H. Schonbacher

Canada Wire and Cable Limited
Power & Control Products Division
22 Commercial Road
Toronto, Ontario
CANADA M4G 1Z4
Attn: Z. S. Paniri

Centro Elettrotecnico
Sperimentale Italiano
Research and Development
Via Rubattino 54
20134 Milan,
ITALY
Attn: Carlo Masetti

Commissariat a l'Energie Atomique
ORIS/LABRA
BP N° 21
91190 Gif-Sur-Yvette
FRANCE
Attn: G. Gaussens
J. Chenion
F. Carlin

Commissariat a l'Energie Atomique
CEN Cadarche DRE/STRE
BP N° 1
13115 Saint Paul Lez Durance
FRANCE
Attn: J. Campan

Conductores Monterrey, S. A.
P.O. Box 2039
Monterrey, N. L.
MEXICO
Attn: P. G. Murga

Electricite de France
(S.E.P.T.E.N.)
12, 14 Ave. Dubrieroz
69628 Villeurbarnie
Paris, FRANCE
Attn: H. Herouard
M. Hermant

Electricite de France
Direction des Etudes et Recherches
1, Avenue du General de Gaulle
92141 CLAMART CEDEX
FRANCE
Attn: J. Roubault
L. Deschamps

Electricite de France
Direction des Etudes et Recherches
Les Renardieres
Boite Postale n° 1
77250 MORET SUR LORING
FRANCE
Attn: Ph. Roussarie
V. Deglon
J. Ribot

Energia Nucleare e delle
Energie Alternative
CKE Casaccia
1-0060 Rome
ITALY
Attn: A. Cabrini

EURATOM
Commission of European Communities
C.E.C. J.R.C.
21020 Ispra (Varese)
ITALY
Attn: G. Mancini

FRAMATOME
Tour Fiat - Cedex 16
92084 Paris La Defense
FRANCE
Attn: G. Chauvin
E. Raimondo

Furukawa Electric Co., Ltd.
Hiratsuka Wire Works
1-9 Higashi Yawata - 5 Chome
Hiratsuka, Kanagawa Pref
JAPAN 254
Attn: E. Oda

Gesellschaft fur Reaktorsicherheit
(GRS) mbH
Glockengasse 2
D-5000 Koln 1
WEST GERMANY
Attn: Library

Health & Safety Executive
Baynards House
1 Chepstow Pl, Westbourne Grove
London W2 4TF
ENGLAND
Attn: W. W. Ascroft-Hutton

ITT Cannon Electric Canada
Four Cannon Court
Whitby, Ontario L1N 5V8
CANADA
Attn: B. D. Vallillee

Imatran Voima Oy
Electrotechn. Department
P.O. Box 138
SF-00101 Helsinki 10
FINLAND
Attn: B. Regnell
K. Koskinen

Institute of Radiation Protection
Department of Reactor Safety
P.O. Box 268
00101 Helsinki 10
FINLAND
Attn: L. Reiman

ISMES S.p.A.
Viale G. Cesare, 29
24100 BERGAMO, Italy
Attn: A. Castoldi
M. Salvetti

Japan Atomic Energy Research
Institute
Takasaki Radiation Chemistry
Research Establishment
Watanuki-machi
Takasaki, Gunma-ken
JAPAN
Attn: N. Tamura
K. Yoshida
T. Seguchi

Japan Atomic Energy Research
Institute
Tokai-Mura
Naka-Gun
Ibaraki-Ken
319-11, JAPAN
Attn: Y. Koizumi

Japan Atomic Energy Research
Institute
Osaka Laboratory for Radiation
Chemistry
25-1 Mii-Minami machi,
Neyagawa-shi
Osaka 572
JAPAN
Attn: Y. Nakase

Kalle Niederlassung der Hoechst AG
Postfach 3540
6200 Wiesbaden 1,
WEST GERMANY
Biebrich
Attn: Dr. H. Wilski

Kraftwerk Union AG
Department R361
Hammerbacherstrasse 12 + 14
D-8524 Erlangen
WEST GERMANY
Attn: I. Terry

Kraftwerk Union AG
Section R541
Postfach: 1240
D-8757 Karlstein
WEST GERMANY
Attn: W. Siegler

Kraftwerk Union AG
Hammerbacherstrasse 12 + 14
Postfach: 3220
D-8520 Erlangen
WEST GERMANY
Attn: W. Morell

Motor Columbus
Parkstrasse 27
CH-5401
Baden
SWITZERLAND
Attn: H. Fuchs

National Nuclear Corporation
Cambridge Road, Whetstone
Leicester LE8 3LH
ENGLAND
Attn: A. D. Hayward
J. V. Tindale

NOK AG Baden
Beznau Nuclear Power Plant
CH-5312 Doettingen
SWITZERLAND
Attn: O. Tatti

Norsk Kabelfabrik
3000 Drammen
NORWAY
Attn: C. T. Jacobsen

Nuclear Power Engineering Test Center
6-2, Toranomon, 3-Chome
Minato-ku, #2 Akiyana Bldg.
Tokyo 105
JAPAN
Attn: K. Takumi

Ontario Hydro
700 University Avenue
Toronto, Ontario M5G 1X6
CANADA
Attn: R. Wong
B. Kukreti

Oy Stromberg Ab
Helsinki Works
Box 118
FI-00101 Helsinki 10
FINLAND
Attn: P. Paloniemi

Radiation Center of
Osaka Prefecture
Radiation Application-
Physics Division
Shinke-Cho, Sakai
Osaka, 593, JAPAN
Attn: S. Okamoto

Rappinl
ENEA-PEC
Via Arcoveggio 56/23
Bologna
ITALY
Attn: Ing. Ruggero

Rheinisch-Westfallscher
Technischer Uberwachunge-Vereln
e.V.
Postfach 10 32 61
D-4300 Essen 1
WEST GERMANY
Attn: R. Sartori

Sydkraft
Southern Sweden Power Supply
21701 Malmo
SWEDEN
Attn: O. Grondalen

Technical University Munich
Institut for Radiochemie
D-8046 Garching
WEST GERMANY
Attn: Dr. H. Heusinger

UKAEA
Materials Development Division
Building 47
AERE Harwell
OXON OX11 ORA
ENGLAND
Attn: D. C. Phillips

United Kingdom Atomic Energy
Authority
Safety & Reliability Directorate
Wigshaw Lane
Culcheth
Warrington WA3 4NE
ENGLAND
Attn: M. A. H. G. Alderson

Waseda University
Department of Electrical
Engineering
3-4-1 Ohkubo, Shinjuku-ku
Tokyo 160
JAPAN
Attn: Y. Ohki

Sorrento Electronics
General Atomic Company
P.O. Box 81608
San Diego, CA 92138
Attn: T. Moshenrose

Toledo Edison Company
NFED-EQ
Mail Stop 3040
5501 North S.R. 2
Oak Harbor, OH 43449
Attn: Peter W. Jacobsen

Office of Scientific and Technical Information
P.O. Box 62
Oak Ridge, TN 37831 (8)

1200 J. P. VanDevender
1234 G. J. Lockwood
1512 J. A. Lewin
1800 R. L. Schwoebel
1810 R. G. Kepler
1811 R. L. Clough
1812 J. M. Zeigler
1812 K. T. Gillen
1813 J. G. Curro
2126 J. E. Gover
2126 O. M. Stuetzer
2514 L. L. Bonzon
3141 S. A. Landenberger (5)
3151 W. L. Garner
6200 V. L. Dugan
6221 E. H. Richards (7)
6258 P. M. Drozda
6300 R. W. Lynch
6400 D. J. McCloskey
6420 J. V. Walker
6429 K. D. Bergeron
6440 D. A. Dahlgren
6442 W. A. Von Riesemann
6447 W. H. Buckalew
6447 L. D. Bustard
6447 M. J. Jacobus (10)
6447 D. L. Berry
6447 M. P. Bohn
6511 F. V. Thome
6512 F. J.Wyant
8524 P. W. Dean

NRC FORM 335 (2-84) NRCM 1102, 3201, 3202

SEE INSTRUCTIONS ON THE REVERSE

U.S. NUCLEAR REGULATORY COMMISSION

BIBLIOGRAPHIC DATA SHEET

1 REPORT NUMBER (Assigned by TIDC and Vol. No., if any)

NUREG/CR-4728
SAND86-1938

2 TITLE AND SUBTITLE

EQUIPMENT QUALIFICATION RESEARCH TEST OF A HIGH-RANGE RADIATION MONITOR

3 LEAVE BLANK

4 DATE REPORT COMPLETED

MONTH	YEAR
January	1988

5 AUTHOR(S)

E. H. Richards, M. J. Jacobus
P. M. Drozda and J. A. Lewin

6 DATE REPORT ISSUED

MONTH	YEAR
February	1988

7 PERFORMING ORGANIZATION NAME AND MAILING ADDRESS (Include Zip Code)

Sandia National Laboratories
Albuquerque, NM 87185-5800

8 PROJECT/TASK/WORK UNIT NUMBER

9 FIN OR GRANT NUMBER

A1051

10 SPONSORING ORGANIZATION NAME AND MAILING ADDRESS (Include Zip Code)

Division of Engineering
Office of Nuclear Regulatory Research
U.S. Nuclear Regulatory Commission
Washington, DC 20555

11a TYPE OF REPORT

b PERIOD COVERED (Inclusive dates)

12 SUPPLEMENTARY NOTES

13 ABSTRACT (200 words or less)

A high-range radiation detector was tested in a simultaneous steam and radiation environment simulating a postulated loss-of-coolant accident (LOCA) to assess possible synergistic effects that may be important to its performance in an accident. The detector, manufactured by General Atomic, was simultaneously subjected to a simulated accident environment including 171°C (340°F) steam at 410 kPa gage (60 psig) and 4 Mrad/hr gamma radiation while its performance was monitored. Test results showed that the detector successfully operated at the high dose rate and temperature, without evidence of synergisms. However, at reduced radiation levels in a saturated steam environment, the detector signal at the readout module deteriorated in accuracy or ceased altogether. The cause of these anomalies is attributed to leakage currents and/or possible galvanic action in the coaxial connections and/or cables.

14 DOCUMENT ANALYSIS - a KEYWORDS/DESCRIPTORS

b IDENTIFIERS/OPEN-ENDED TERMS

15 AVAILABILITY STATEMENT

Unlimited

16 SECURITY CLASSIFICATION

(This page)
Unclassified
(This report)
Unclassified

17 NUMBER OF PAGES

64

18 PRICE

☆ U.S. GOVERNMENT PRINTING OFFICE: 1988—573-049/61044

120555078877 1 1AN1RV
US NRC-OARM-ADM
DIV OF PUB SVCS
POLICY & PUB MGT BR-PDR NUREG
W-537
WASHINGTON DC 20555